SENSORY CODING OF COMPLEX VISUAL MOTION IN THE LOCUST (*Locusta migratoria)*

A Thesis Submitted to the College of Graduate

Studies and Research in Partial Fulfillment of the

Requirements for the Degree of Master of Science

in the Department of Biology

University of Saskatchewan

Saskatoon

By

Paul Cameron Dick

PERMISSION TO USE

In presenting this thesis in partial fulfillment of the requirements for a Postgraduate degree from the University of Saskatchewan, I agree that the Libraries of this University may make it freely available for inspection. I further agree that permission for copying of this thesis in any manner, in whole or in part, for scholarly purposes may be granted by the professor or professors who supervised my thesis work or, in their absence, by the Head of the Department or the Dean of the College in which my thesis work was done. It is understood that any copying or publication or use of this thesis or parts thereof for financial gain shall not be allowed without my written permission. It is also understood that due recognition shall be given to me and to the University of Saskatchewan in any scholarly use which may be made of any material in my thesis.

Requests for permission to copy or to make other uses of materials in this thesis in whole or part should be addressed to:

Head of the Department of Biology
University of Saskatchewan
Saskatoon, Saskatchewan, S7N 5E2
Canada

OR

Dean
College of Graduate Studies and Research
University of Saskatchewan
107 Administration Place
Saskatoon, Saskatchewan, S7N 5A2
Canada

ABSTRACT

The visual environment of any animal is a complex amalgamation of sensory information (Lochmann and Deneve, 2011); however, it is adaptive for an animal to only react to salient cues (Zupanc, 2010). For many organisms, the detection of an approaching object, such as an oncoming conspecific or a predator, is particularly important. An approaching object with constant velocity is called looming, and has been widely studied for evoking avoidance behaviours in a number of animal species (Gibson, 1958). The migratory locust, *Locusta migratoria,* has been used extensively as a model system for visually guided behaviour, due to its robust collision-avoidance behaviours and its tractable nervous system (Schlotterer, 1977). The Lobula Giant Movement Detector (LGMD) and the Descending Contralateral Movement Detector (DCMD) constitute one pathway in the locust visual system that integrates the entire field of view that has been implicated in coordinating these types of behaviours (Santer et al., 2006).

Previous studies have found that the LGMD/DCMD pathway responds to many visual stimuli, including complex scenes (Rind and Simmons, 1992), approaching paired objects (Guest and Gray, 2006), objects with compound shapes (Guest and Gray, 2006), and objects that follow compound trajectories (McMillan and Gray, 2012). These findings suggest that this pathway is capable of encoding complex motion such as exists in the locust's natural environment. In my first objective (Chapter 2), I tested the response of the locust DCMD to increasingly complex motion. Using computer generated disks that followed compound trajectories with different velocities, I demonstrate that the DCMD is capable of encoding the location, trajectory, and velocity of an approaching object through aspects of the response profile over time.

The motor systems of invertebrates are often controlled by ensembles of neurons working together (Dubuc et al., 2008; Hedrich et al., 2011; Gonzalez-Bellido et al., 2013). The locust visual system has at least five identified descending neurons, beyond the DCMD, that respond to visual motion (Rowell, 1971; Griss and Rowell, 1986; Gray et al., 2010). Due to the tractability of extracellular recordings of the DCMD, these neurons remain relatively little studied. Furthermore, their responses to stimuli have not been investigated concurrently. With recent advancements in multichannel recordings and spike sorting algorithms, it is now possible to explore the responses of multiple neurons in the locust system together. In my second objective (Chapter 3), I recorded from the connective of the locust using multichannel electrodes while challenging it with a wide array of visual stimuli. Preliminary results of these experiments identified as many as five neuronal units with distinctive firing patterns, some which appear to be novel.

Together, these results illustrate that the locust visual system is more complex than previously thought, through both the abilities of a single neuron to encode many aspects of visual motion and the presence of multiple unique, visually-sensitive neurons.

ACKNOWLEDGEMENTS

First, I am grateful to my supervisor, Dr. John (Jack) Gray. From introducing me to the exciting world of physiology and neuroethology in my undergraduate to supervising an undergraduate research project, a summer project, and a Master's project, he has had a profound impact on my University career. Second, I have to recognize the support of Glyn McMillan. First as lab coordinator and later as lab manager, he has helped me through the many frustrations of data analysis and interpretation. His proofreading skills have also proven invaluable, as have the after-work unwind beers. I am also grateful to the rest of my labmates, for the help and support over the last few years.

I would like to thank Drs. Tracy Marchant and John Howland for serving as members of my committee. Their input and direction have been invaluable. I would also like to thank the Biology Department as a whole, for providing me with the opportunity and funding to explore my interests and introducing me to a wide array of people whom I would not have had the chance to meet otherwise. I'm especially thankful for the chance to help teach undergraduate students, one of the most enjoyable aspects of my own career as a student.

Thank you to all of my friends and family- I know it has not been easy to feign interest in my research, and I appreciate the relative dearth of eye rolling and snores. Mom and Dad, Sarah and Cameron Dick, you have always been supportive of my choices in life, even if those choices took me a province away with no prospect of going back (I swear, it's beautiful in the summer!). I hope you learned a little bit of biology from my ramblings. Finally, I want to deeply thank Kristine Hunter, who has put up with more than the rest combined, yet continues to support me. I would not be here without you.

TABLE OF CONTENTS

LIST OF FIGURES

LIST OF ABBREVIATIONS

$\|v\|$	- Absolute Velocity
2D	- 2 Dimensional
b	- y-Intercept
CNS	- Central Nervous System
DCMD	- Descending Contralateral Movement Detector
DIMD	- Descending Ipsilateral Movement Detector
DNC	- Contralateral Deviation-Detector Neuron
DNI	- Ipsilateral Deviation-Detector Neuron
DNM	- Medial Deviation-Detector Neuron
f	- Firing Rate
f'	- Change in Firing Rate
l	- Half Size
LDCMD	- Late Descending Contralateral movement Detector
LGMD	- Lobula Giant Movement Detectors
m	- Slope
PCC	- Pearson Product-Moment Correlation
png	- Portable Network Graphic
PSTH	- Peristimulus Time Histogram
R cells	- Retinula Cells
SD	- Standard Deviation
T90	- Time that an object crossed 90° azimuth

TOC - Time of Collision

TOT - Time of Transition

vsync - Vertical Refresh Synchronization Pulse

δ - Response Delay

θ - Subtense Angle

θ'' - Instantaneous Angular Acceleration of the Subtense Angle

ψ - Angle of the Leading Edge

ψ'' - Instantaneous Angular Acceleration of the Leading Edge

CHAPTER 1

GENERAL INTRODUCTION AND LITERATURE REVIEW

1.1 NEUROETHOLOGY

Neuroethology is the study of the neural mechanisms that underlie natural animal behaviour (Zupanc, 2010). While neuroethologists historically focused on exhaustively exploring the neuranatomy of a system, the discoveries of neuromodulators which change neuronal function (Harris-Warrick and Marder, 1991) and neurons with multiple roles (Hooper and Moulins, 1989) have shifted popularity to a "top-down" approach. By using stereotyped behaviours with dissected, minimalist stimuli, researchers are able to identify the underlying neural mechanisms. Moreover, by incrementally manipulating and increasing the complexity of the stimulus, the underlying computational rules can be better understood, with the eventual creation of biologically-relevant models of animal behaviour.

1.2 PRINCIPLES OF SENSORY CODING

1.2.1 Sensory Environments

The natural environment of an animal is complex, an amalgamation of incomplete, noisy, and ambiguous information (Lochmann and Deneve, 2011). Modern computers, which reliably beat the best chess players in the world, still cannot manipulate objects or understand visual scenes at even the level of a toddler. This disparity is largely a result of animals developing, over the course of evolution, solutions to their common problems that are close to optimal (Körding, 2007). The connection between perception of the environment and initiation of relevant

behaviours is often described using Bayesian models (Ernst and Banks, 2002; Daw et al., 2006; Clemens et al., 2011); though the sensory information available to an animal may not be complete, weighted analysis of what is available will often result in accurate decision making. Many animal systems have evolved the ability to extract specific, behaviourally relevant features of their environment. For example, neurons in the visual system of the crab, *Uca vomeris,* can distinguish an approaching predator from flickering in light intensity (such as produced by beating wings) and retinal speed, both of which affect their escape responses (Hemmi and Tomsic, 2012). The visual system of the crab is relatively simple, yet is capable of producing a robust and relevant behavior that can be critical for survival. A rapidly approaching object evokes avoidance behaviours that have been studied in many animal species (Gibson, 1958). The locust is an example of a well-studied organism in which visual information alone will trigger adaptive behavioural responses (Robertson and Johnson, 1993a; Gabbiani et al., 2001; Gray et al., 2001; Santer et al., 2006). As a flying, diurnal insect, the visual environment of the locust includes motion caused both by movement of the individual itself and the motion of other animals, which includes conspecifics and predators. Detection of approaching objects and initiation of rapid responses in such a complex visual environment is highly adaptive (Baker et al., 1981). To understand these responses, both at the level of the behaviour and the underlying neuronal mechanism, we must be able to identify the salient aspects of the environment.

1.2.2 Sensory Coding

Neuronal firing can display one of two binary states, the presence or absence of an all-or-nothing action potential (Stein et al., 2005), the pattern of which contains information with

varying degrees of complexity (Panzeri et al., 2010). This pattern of action potentials is called the neural code, and in sensory neurons it encodes a representation of the external or internal environment of an organism (Ferster and Spruston, 1995). In general, a specific neural code is described by two components: the spacial dimension is the distribution of neurons within a nervous system, while the temporal dimension is the response of neurons over time. Through interactions of these two dimensions, neurons are capable of transmitting vast amounts of information and controlling complicated behaviours.

Many neurons encode information through an averaged firing rate, which is referred to as a rate code (Mehta et al., 2002). While this form of code can provide accurate representation of inputs, they are often averaged over hundreds of milliseconds, whereas synaptic efficacy may require precise timing of spikes, within 10 ms (Markram et al., 1997). These small time-scale changes in neuronal activity may be incorporated into a temporal code. Through exactly timed increases in activity across multiple, spatially related neurons, sequential and simultaneous firing can encode additional parameters of the sensory inputs (Elhilali et al., 2010). Temporal codes also exist within single neurons; latency, the delay between stimulus and response, is thought to code intensity in electrolocation of mormyrid fish (Hall et al., 1995) and direction of whisker deflection in rats (Storchi et al., 2012). The interspike interval, or timing between spikes, can also be used to code sensory information (Chase and Young, 2007), and has been implicated in encoding spatial structure in retinal ganglion cells (Gollisch and Meister, 2008) as well as head direction in rats (Taube, 2010). A phase-of-firing code requires multiple neurons, including some form of background oscillation. These encode information through spike times in one neuron relative to the phase of the oscillator, and are being found to facilitate functions such as learning (Masquelier et al., 2009) and memory (Lisman and Jensen, 2013) in addition to encoding sensory

information (Huxter et al., 2008).

The forms of neural code discussed so far have been addressed as separate entities; however, combining codes over different timescales within a single pathway can increase the capacity for information to a level capable of encoding the true sensory world (Panzeri et al., 2010). These are known as multiplexed codes, and are increasingly being associated with many neural processes. Combinations of rate and temporal codes provide robust representations of auditory stimuli in ferrets (Walker et al., 2011), vibrations in human fingertips (Harvey et al., 2013), three-dimensional motion in primates (Huk, 2012), and memories in the human cortex (Knight and Eichenbaum, 2013). Currently, multiplexed codes are most often applied to higher-order organisms, such as primates or other mammals. While there has been some evidence of bursting, brief episodes of high-frequency firing that form a multiplexed code, in insect systems (Marsat and Pollack, 2006), invertebrates have a dearth of relevant studies. While this can be attributed to a delay in technical advances to make such studies possible, it is a lack that must be addressed. Multiplexed codes are capable of containing information that is only available when all temporal scales are combined, so it is crucial that we understand whether multiplexing occurs if we aim to correctly describe invertebrate sensory systems.

1.2.3 Neuronal Ensembles

The previous section described mechanisms of encoding sensory information which involves only one or a few neurons. Early single-neuron research, which focused on these methods, went so far as to suggest that irregularity in neuronal activity, which is commonly observed in recordings, was simply noise that needed to be removed or averaged out to

understand the underlying code (Shadlen and Newsome, 1998). In contrast, it has been theorized that much of the information held in a nervous system is represented in populations made of large numbers of neural elements (Freeman, 1995). Recent advances in multichannel recordings and analysis techniques have allowed researchers to simultaneously record from large numbers of neurons, producing the clearest picture to date of what occurs in neural systems. The most common technique is to use multichannel electrodes which provide localized parallel recordings from multiple neurons (Buzsáki, 2004). The magnitude of a recorded spike is a function of, amongst other factors, the distance between the neuron and the electrode (McNaughton et al., 1983). By recording from multiple sites, it is possible to discriminate individual units based on spike timing and magnitude across electrodes. Furthermore, if the electrodes are distributed across three dimensions, it is possible to triangulate the location of the neuron as well as determine the direction of conductance (i.e. efferent or afferent). These multichannel electrodes provide numerous advantages, including larger unit yields, mechanical stability over single tip electrodes, and increased applicability to long-term recordings (due to the ability to identify neurons from a greater distance) (Buzsáki, 2004).

Neuronal ensembles are thought to provide more information than possible with small-scale codes (Buzsáki, 2004), and in a more energy efficient manner (Laughlin and Sejnowski, 2003). Recent studies have implicated neuronal networks in systems such as the visual (Shadlen and Newsome, 1998) and auditory cortex (O'Connell et al., 2011) of monkeys, position prediction (Brown et al., 1998) and both spatial and episodic memory (Leutgeb et al., 2005) in the rat hippocampus, and disruption of ensembles is thought to be related to Alzheimer's disease (Palop and Mucke, 2010). In invertebrates, motor behaviours are often controlled by populations of neurons (Dubuc et al., 2008; Hedrich et al., 2011; Gonzalez-Bellido et al., 2013), while other

species have parallel pathways controlling similar behaviours (Eaton et al., 2001; Fotowat et al., 2009). As analytical methods are improved, it is becoming evident that few systems do not include some form of interaction between neurons. To fully understand how these systems function, it is critical to describe these interactions.

1.3 INSECT VISION

Since the first characterization of the compound eye by van Leuwenhoek 300 years ago, insect vision has attracted biologists and physicists endeavoring to understand these systems (Borst, 2009). With modern technological advancements, such as the ever-expanding genetic toolkits, we have a more clear understanding of compound eyes than we ever have before. The compound eye of an insect is made of many repeating units called ommatidia (Land and Nilsson, 2012). The outermost part of each ommatidium is a corneal lens, also known as a facet, which lies over the crystalline cone; these structures together form the dioptric apparatus and focus photons on to the underlying photoreceptors, the retinula cells (R cells) (Fig. 1.1). Each ommatidium contains 8-9 R cells which contain photon-absorbing visual pigments arranged in microvilli called rhabdomeres. The rhabdomeres are fused together to form the light-sensitive rhabdom through the central axis of the ommatidia. Different cell types contain different types of pigment; primary pigment cells surround the crystalline cone, secondary pigment cells ensheath the ommatidium as a whole, and retinula cell pigments are contained within R cells.

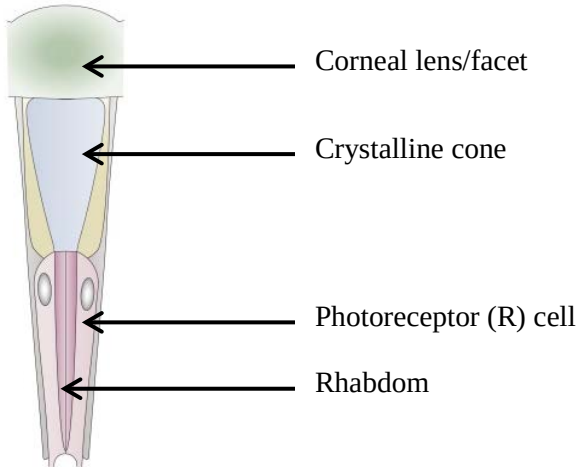

Figure 1.1: Semischematic model of a single insect ommatidium. Light enters the ommatidium through the cornea and crystalline cone, which focus the light onto the rhabdom. The rhabdom is the light sensing apparatus, which synapses on to the optic nerve. Modified from Nilsson and Kelber,(2007, Fig. 1).

When photons are absorbed by a photoreceptive pigment, the energy is converted into an electrical response via the gating of ion channels. This phototransduction can amplify the microscopic activation of a single rhodopsin molecule by a photon of light in to the gating of about 1000 ion channels in vertebrates and 10,000 ion channels in insects (O'Day et al., 1997). A single photon incident on the microvilli of the photoreceptive cells will trigger the opening of channels; in insects, a single channel may be sufficient to generate a detectable response (Hardie, 2001). These unique properties mean that insect vision is incredibly sensitive to local, small-field motion.

There are two general forms of compound eyes found in insects. Apposition eyes are the most common, and are distinguished by independent ommatidia, with each facet only refracting light to the rhabdom of its respective ommatidium (Fig. 1.2). In superposition eyes, visual information converges at the eye. Neural superposition eyes are similar in anatomy to apposition

compound eyes, but with unfused rhabdomeres that each receives light from a slightly different angle. The axons of photoreceptors from six adjacent ommatidia with the same field of view then converge onto the same cartridge (Kirschfeld, 1967). Non-neural superposition eyes contain a "clear zone" that spatially separates the facet from the rhabdom. Light that enters the facet is redirected, through either refraction or reflection, to be incident on multiple photoreceptors, with each rhabdom receiving light from hundreds to thousands of facets. The convergence of visual information improves the sensitivity of all superposition eyes, at the detriment of resolution (Caveney and McIntyre, 1981). This provides a huge advantage in low light environments, and thus is found most commonly in nocturnal invertebrates. Diurnal insects, especially those who rarely fly in low levels of light such as the locust, gain no benefit from the increased sensitivity, and so have evolved the higher resolution apposition eye.

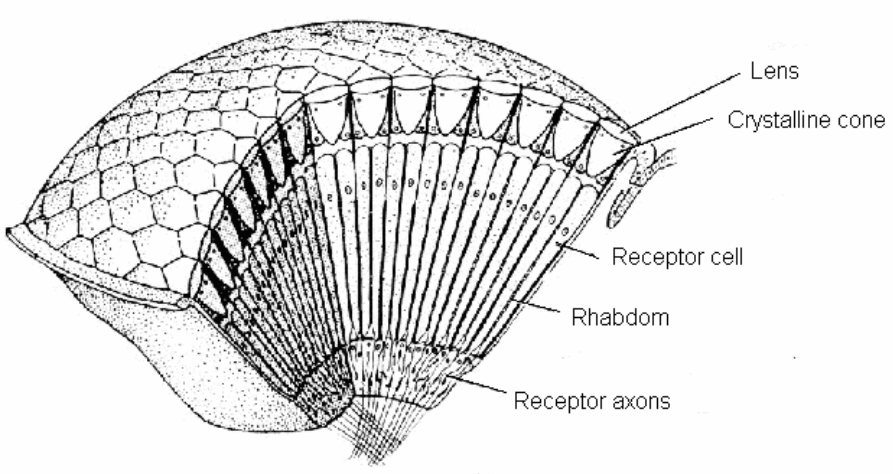

Figure 1.2: Semischematic model of an apposition type of compound eye. The apposition compound eye is made up of many separate ommatidia. Each ommatidium is at a different angle, which allows for a wide field of view (Burrows 1996). Modified from Land and Nilsson (2002, Fig. 7.3).

1.4 *LOCUSTA MIGRATORIA*

1.4.1 Locust Biology

The migratory locust (*Locusta migratoria*) belongs to the family Acrididae in the order Orthoptera. They are pests native to Africa, Japan, Australia, and the Phillipines (Chapman, 1976). Locusts exist in two morphologically and behaviourally distinct phases, gregarious and solitarious (Matheson et al., 2004). Locusts in the solitary phase live singly or in small groups with densities less than 3 per 100 m^2, fly less frequently, only short distances, and typically at night (Matheson et al., 2004). An increase in population density triggers a switch to the gregarious phase, primarily due to increased mechanical stimulation to the hind legs by conspecifics in close proximity (Simpson et al., 2001), resulting in the upregulation of certain metabolic pathways (Ma et al., 2011). Behavioural changes (i.e. swarming) can take as little as an hour to develop, while morphological changes take longer: colour changes take one generation, while shape changes can take two or more generations to develop (Roessingh et al., 1993). Gregarious locusts form large, migratory swarms with densities as high as 100,000 per km^2 (Matheson et al., 2004) that travel over 10 km in an hour, with individual flight speeds of 3-6 m/s (Robertson and Johnson, 1993a). These swarms can be devastating to local agriculture; it has been estimated that swarms of *Schistocerca gregaria*, the desert locust, affect 20% of the land in the world and 10% of the global human population (Burrows, 1996). An outbreak of *Locusta migratoria* in Madagascar in 2013 is expected to cost over $40 million dollars to control, and threatens 60% of the country's crops.

1.4.2 *Locusta* as a Model System

The choice of a model system for study is often difficult for neuroethologists, as the complexity of a behavior is usually related to the complexity of the underlying nervous system (Zupanc, 2010). However, due to the pressure of natural selection, some animal systems have evolved behaviours that are similar to higher order organisms, but are carried out using relatively simple nervous systems. Insects in particular are great examples of this. They often exhibit behaviours that are analogous to those in other organisms, but are driven by a small number of individually identifiable neurons. Study of these neurons can yield the general properties and mechanisms used in other systems. In contrast, the neurons in many vertebrate nervous systems are only identifiable as a particular class, rather than an individual neuron. In addition, a great neuroethological model system has other useful qualities including the ease of breeding in captivity and a body of research to build upon.

Locusta migratoria is a neuroethological model system for vision that exemplifies all of these criteria. As a diurnal, swarming insect, the locust depends on vision to avoid both conspecifics flying in close proximity (Simpson et al., 2001) and approaching predators (Guest and Gray, 2006). These extreme selection pressures have driven the evolution of precise collision avoidance behaviours, which are thought to be primarily driven by as few as three major interneurons (Gray et al., 2010). The flight motor system of the locust has been well defined anatomically (Snodgrass, 1929; Marden, 2000) and physiologically in the context of flight (Campbell, 1961; Wilson and Weis-Fogh, 1962; Wolf, 1993; Shoemaker and Robertson, 1998). The behavioural response of the locust has been particularly well studied for a number of different stimuli, including acoustic (Dawson et al., 1997), thermal (Robertson et al., 1996; Shoemaker and Robertson, 1998), and visual stimuli (Robertson and Johnson, 1993a; Santer et

al., 2004; Gray, 2005; Rogers et al., 2010; McMillan et al., 2013). The expansive knowledge base for locusts and the relative ease of use as a laboratory specimen make *Locusta migratoria* an excellent neuroethological model system, with the potential to describe many of the mechanisms that underlie vision in all animals.

1.4.3 Anatomy and physiology

Locusta, like all insects, have a hard, jointed exoskeleton made of cuticle formed in to either hard plates, called sclerites, or flexible membranes. The dorsal sclerites, or tergum, are joined to the ventral sclerite, the sternum, by the pleura, a membranous area lateral on the body. Jointed appendages grow from the sternopleaural region on each side of the body. The segments of the body are grouped into three units, the head, thorax, and abdomen, in which the basic parts are modified or lost completely.

The head of the locust is connected to the thorax by a flexible, membranous neck. It includes the mouthparts and sense organs including the antennae, compound eyes, and ocelli. The antennae contain many sensilla, including mechanosensory hairs, chemoreceptors for olfaction, and the base, or pedicel, contains a chordotonal organ, which responds to movement of the flagellum as a whole (Chapman, 1998). The ocelli are crude photoreceptive organs, whose function is uncertain; they appear to be adapted to perceive changes in light intensity, and in the locust are implicated in detecting roll and position of the horizon (Simmons, 1993). The compound eye of the locust is of the apposition type, as discussed in more detail above.

The thorax of the locust is separated in to three segments, the pro-, meso- and meta-thoracic segments. Each segment bears a pair of legs, with a pair of wings on both of the meso-

and meta-thoracic segments. These segments are more heavily muscled, to provide the force necessary for locomotion. The tergum of the prothoracic segment is called the pronotum. The abdomen of a locust has 11 visible segments in addition to the posterior telson. These segments have no appendages other than those involved with reproduction. The surface of the abdomen has mechanosensitive sensilla, and grasshoppers, including locusts, have chemoreceptors scattered amongst the mechanoreceptors (Thomas, 1965).

1.4.3.1 Nervous System

The basic element of the nervous system is the neuron, which are most commonly monopolar with only a single projection from the soma that branches to form both the axon and dendrite (Burrows, 1996). Exceptions to this are peripheral sense cells, which are often bipolar with a short dendrite receiving sensory information, and multiplolar ganglial cells, associated with stretch receptors. Nutrient-providing glial cells enfold the neurons, with gaps allowing synaptic contacts (Carlson and Saint Marie, 1990). A specialized layer of glial cells, known as the perineurium, surround the entire central nervous system (CNS) and the larger peripheral nerves. These cells are held together by tight junctions and desmosomes, forming a blood-brain barrier that protects the neural environment. The cells of the perineurium excrete mucopolysaccharides and mucoproteins with collagen-like fibrils which form a thick basal lamina known as the neural lamella. Together, the perineurium and neural lamella are known as the nerve, or neural, sheath.

The CNS consists of the brain, located dorsally in the head, and a series of segmental ganglia above the ventral body wall (Burrows, 1996). The somata within ganglia are grouped

peripherally, with the center of each ganglion occupied by the terminal end of sensory axons, the dendrites of motor neurons, and the axons of interneurons. This mass of fibers is known as the neuropil, and is the location of synapses between neurons; other than the neuromuscular junction, no synapses occur outside the CNS (Altman and Kien, 1987). Ganglia are joined by interganglionic connectives containing only axons and glia. The locust contains a total of nine ganglia, beginning with the subesophageal ganglion directly posterior the brain which controls the mouthparts. This is followed by three thoracic ganglia, with five or six nerves branching on each side to innervate muscles and sensilla of the thorax. The abdomen of the locust contains five ganglia, which are smaller in size and have fewer peripheral nerves (Chapman, 1998).

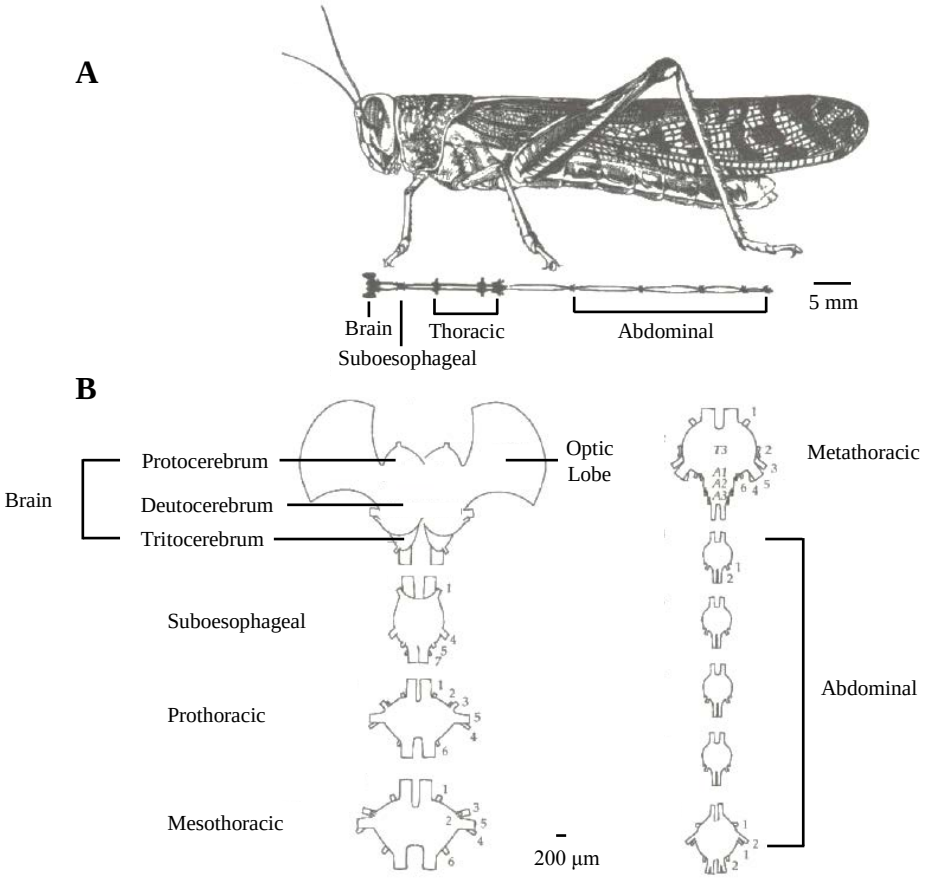

Figure 1.3: The central nervous system of a locust consists of the brain and nine ganglia, (A) A drawing of a locust and a scale drawing of its nervous system. (B) Drawings of the regions of the brain and ganglia. Numbers indicate neuromeres. Figure modified from Burrows (1996).

The brain is the principal association center of the body, receiving sensory input directly from sense organs of the head and indirectly from the ganglia. Few motor neurons are present in the brain, and are mainly responsible for antennal muscles; the majority of the cell bodies belong to interneurons involved with integrating neural activity. The brain consists of three regions: the protocerebrum, deutocerebrum, and tritocerebrum (Fig. 1.3B). The protocerebrum is bilobed, lateral to the optic lobes with peripherally oriented somata with an interior neuropil. The anteriodorsal region is called the pars intercerebralis, which includes ocellar nerves, neurosecretory cells, and the pons cerebralis acting as a relay hub. This region of the brain also includes the mushroom bodies, a mass of interneurons which receive input from the antennal lobes and are involved in olfaction (Schurmann, 1987). The central complex of the protocerebrum is a series of well-ordered neuropils that are thought to be involved in integration of information between the right and left halves of the brain (Homberg, 1987, 1991).

Expanding laterally from the protocerebrum are the optic lobes, which contain three neuropil masses: the lamina, the medulla, and the lobula complex. Retinula cell axons extend to the lamina, where they are organized in to cartridges by ommatidia. Those that terminate in the lamina synapse with two types of monopolar interneurons that connect to the medulla (Laughlin, 1981). Small-field monopolar cells receive input from only one cartridge, while wide-field monopolar cells receive from multiple cartridges (Gilbert and Strausfeld, 1992). The identity of group and cell is maintained in the medulla, where the pattern of neural signals is a representation of an image on the eye- this is known as retinotopic mapping. The lobula loses some of the precision as pathways converge, relaying particular aspects of the visual stimuli. Interneurons of the lobula are also described as either small-field or wide-field, depending on the number of inputs they receive. Axons from the lobula project to the deutocerebrum, where they

synapse with descending interneurons which regulate motor systems.

The deutocerebrum of the insect contains the olfactory, or antennal, lobe and the antennal motor center (Homberg et al., 1989). The antennal lobe of *Locusta* contains approximately 1000 glomeruli, which receive, process, and relay olfactory information. The final region, the tritocerebrum, is a small pair of lobes underneath the deutocerebtum which act as a relay to and from the subesophageal ganglion (Chapman, 1998).

1.4.3.2 Flight System

The locust flight system is composed of four primary divisions: the thoracic ganglia, proprioceptors of the wings and head, the thoracic flight muscles, and the wings themselves. The thoracic ganglia contain interneurons that make up the motor pattern generator responsible for the basic flight rhythm as well as the motor neurons that convey this rhythm to the flight muscles (Campbell, 1961). Connections between motor neurons and muscles are neurogenic; every action potential from a motor neuron results in the contraction of a flight muscle (Burrows, 1975). This makes the locust system ideal for examining the correlation between behaviour and central neural activity. Proprioceptors, including the tegula (Gettrup, 1966; Wolf, 1993) and the wing hinge stretch receptor (Burrows, 1975; Möhl, 1985) relay wing position to the motor pattern generator to be incorporated in modulation of the rhythm generated. Other proprioceptive input, such as from head-thorax orientation, has been hypothesized to be involved, but is currently not implicated in flight orientation (Miall, 1990; Robert and Rowell, 1992).

Straight flight in locusts is generated though up and down movements of the fore- and hindwings with coordinate twisting of the wing surface controlling lift and drag. Elevation of the

wing is produced by the contraction of medial vertical elevators, which also results in passive elastic supination (movement of the leading edge upward). Depression is produced by a combination of elasticity, dorsal longitudinal depressor muscles (m81 and m112), and a lateral row of vertical depressor muscles (two basalar and one subalar muscles for each the fore- and hindwings). During the downstroke, the hindwing basalar (m127 and m128) and subalar (m129) muscles contract first, followed by the forewing basilar (m97 and m98) and subalar (m99) muscles. These muscles are also responsible for pronation (movement of the leading edge downward) during the downstroke. In total, the muscles responsible for the downstroke of the locust wing contain approximately 10 motor units, each which fire zero, one, or two times. More detailed characterization of the muscles in the locust flight system is provided by Wilson and Weis-Fogh (1962).

In locusts, steering has been thought to require the coordinated response of the abdomen, hindlegs, and wings (Robertson and Reye, 1992). This has been best described in the response to an approaching object. The locust responds to this type of stimulus by turning towards or away from the object (Robertson and Johnson, 1993a; Santer et al., 2006; Rind et al., 2008) or, as a last ditch response, gliding (Santer et al., 2004; McMillan et al., 2013). Variability in avoidance and escape behaviours is observed in many insect species and is thought to be either as a result of perceived threat level (Roeder, 1975), or to preclude anticipation by predators (Domenici et al., 2011; Card, 2012). Recent experiments investigating wing kinematics and muscle activity in loosely tethered locusts described the turning dynamics in more detail (McMillan et al., 2013); see Figure 1.4 for the degrees of freedom of a flying locust. They found that a turn was preceded by a decrease in wing beat frequency, followed by asymmetry in depressor muscle (m97) activity. As a turn is initiated, the yaw angle changes just before the wing beat frequency

increases, coinciding with a shift in forewing asymmetry that changes the roll angle. Shortly after the turn, there is a change in the pitch angle, followed finally by a change in hindwing asymmetry and ruddering of the abdomen. This suggests that abdominal motion is the result of inertia, rather than a controlled movement.

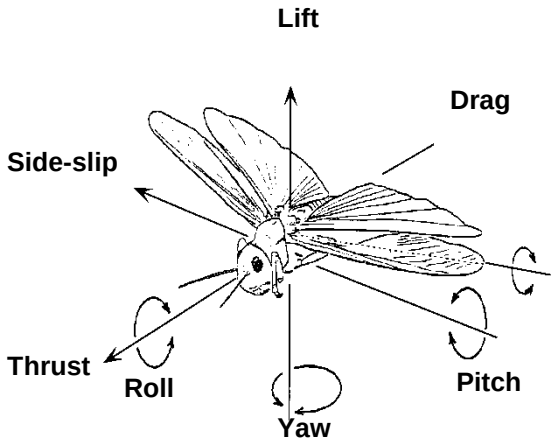

Figure 1.4: Three rotational degrees of freedom (yaw, pitch and roll) and three translational degrees of freedom (thrust/drag, sideslip and lift) of a locust. Figure provided by Indika Perara.

1.4.3.3 Looming Detection

In the natural visual environment of a locust, an object that appears to be on a collision course is of particular importance. This could be a predatory bird diving in for the kill, a conspecific moving closer, or any other object approaching the locust, which likely requires some form of behavioural response. This type of visual motion, an approaching object at constant velocity, is called looming, and is distinguished by the non-linear expansion of the subtense angle during approach (Fig.1. 5). The speed at which the subtense angle increases contains important information about the properties of the approaching object. Looming objects are often characterized by the $l/|v|$ value, a ratio of the half size of the object (l) and its absolute

velocity |*v*| (Gabbiani et al., 1999).

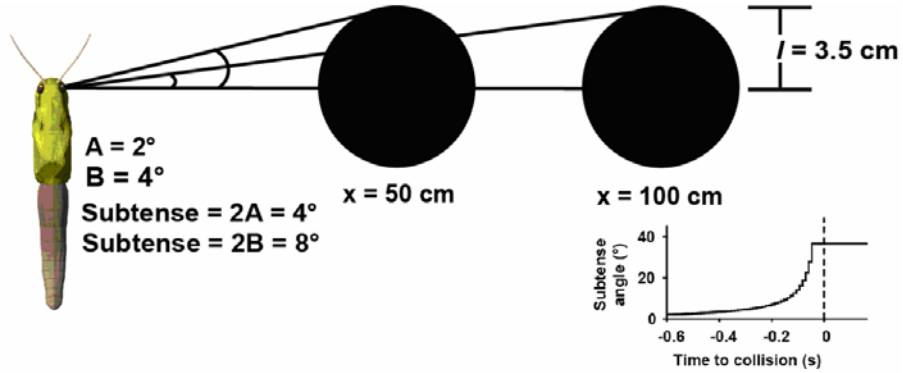

Figure 1.5: Schematic showing the subtense angle on the locust ommatidia of one disk at two positions during a loom. The angle subtended by half of the disk on the locust eye is given for a distance of 100 cm (A) and 50 cm (B); the total subtense angle is double this value. A disk that is closer to the locust with constant size subtends more of the eye. Inset: the subtense angle of a looming disk during a projected loom. The angle increases exponentially until the object ceases motion. Figure provided by Glyn McMillan.

In *Locusta migratoria*, detection of looming begins with the ommatidia, afferents of which synapse with the Lobula Giant Movement Detectors (LGMDs). The visual information is retinotopically integrated into the three dendritic fields of the pair of LGMDs (Peron et al., 2009), where excitation is modulated through a combination of feedforward inhibition and spike-frequency adaptation (Gabbiani et al., 2002). Large and rapid luminance changes cause inhibition of the LGMD (Rowell et al., 1977) through hyperpolarizing postsynaptic potentials produced by two classes of GABAergic neurons (Rind and Bramwell, 1996), creating a feed-forward loop that bypasses processing distal of the LGMD. After the cessation of motion of an approaching object, these inhibitory potentials terminate the excitation of the LGMD (Rind, 1996). Spike-frequency adaptation, thought to be mediated by hyperpolarization as a result of small conductance calcium-dependent potassium channels (Peron et al., 2009), causes a more

intermediate duration adaptation that could result in selectivity of the LGMD response for looming (Gabbiani and Krapp, 2006); translating objects activate a constant number of photoreceptors per unit of time, while a looming object will activate a rapidly increasing number that is sufficient to overcome the adaptation.

The LGMD forms a 1:1 mixed chemical and electrical synapse with The Descending Contralateral Movement Detector (DCMD) receives approximately 8500 identified input synapses, of which at least 2250 are a mixture of gap (electrical) and chemical synapses from the LGMD (O'shea et al., 1974; Killmann et al., 1999). The DCMD decussates at the subesophageal ganglia and continues down to branch in each of the three thoracic ganglia (Burrows and Rowell, 1973), making connections with flight interneurons and motoneurons (Schlotterer, 1977; Simmons, 1980a), implicating this pathway in mediating collision avoidance behaviours.

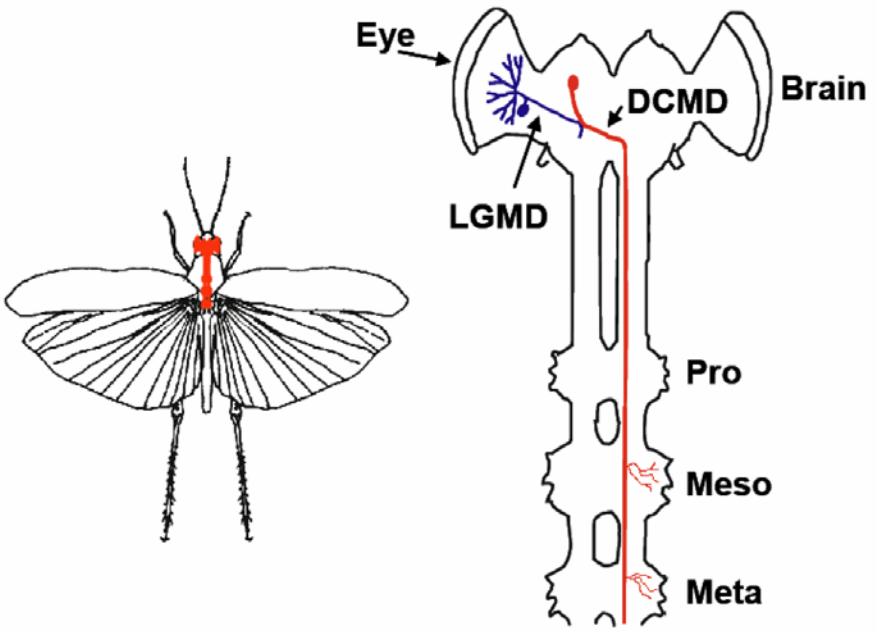

Figure 1.6: Diagram of the locust LGMD/DCMD pathway. Note the crossing of the DCMD from the left eye to the right ventral nerve cord. Figure provided by Dr. John Gray.

The stereotyped response of the LGMD/DCMD pathway to a directly looming object is an increase in firing rate as the object approaches, with a peak just before the time of collision (Fig. 1.7). It is thought that the LGMD performs a multiplicative computation, wherein the dendritic trees multiply the size and velocity signals during object motion through either linear summation with exponential conversion of the dendritic potential in to a firing rate or through shunting inhibition of the velocity by the size (Gabbiani et al., 2002). This results in an increase in firing rate that is related to the $l/|v|$ value of the approaching object (Gabbiani et al., 2002). While the LGMD responds most vigorously to looming objects (Schlotterer, 1977; Gabbiani et al., 1999; Krapp and Gabbiani, 2005), it also responds to small, translating objects (Palka, 1967; Pinter et al., 1982; Peron and Gabbiani, 2009a; McMillan and Gray, 2012). Previous experiments have established that visual information alone can trigger a collision avoidance behaviour in locusts (Robertson and Johnson, 1993b; Santer et al., 2006; Chan and Gabbiani, 2013; McMillan et al., 2013) and that the DCMD responds to complex scenes (Rind and Simmons, 1992), paired approaching objects (Guest and Gray, 2006), objects with compound shapes (Guest and Gray, 2006), and objects following compound trajectories (McMillan and Gray, 2012). These findings strongly suggest that this pathway is capable of encoding complex aspects of visual motion, such as would exist in the locust's natural environment. However, many of the manipulations of visual stimuli have been done in isolation, i.e. a direct loom with different velocities or different directions at the same velocity. To truly understand the abilities of this system, they must be investigated together.

Other visual interneurons have been identified in the locust system, in addition to the DCMD. The late DCMD (LDCMD) responds to looming objects with a profile similar to the DCMD, but with different parameters and weaker habituation to repeated presentations (Gray et al., 2010).

The Descending Ipsilateral Movement Detector (DIMD) appears almost indistinguishable from the DCMD (Fotowat et al., 2009), and is thought to provide redundancy to the system (Santer et al., 2008). Three other neurons, the ipsi-, medial, and contralateral deviation-detector neurons (DNI, DNM, and DNC, respectively; (Griss and Rowell, 1986) respond to large field visual motion (Rowell and Reichert, 1986). These neurons have only been investigated with simple visual stimuli, with the focus on the DCMD and LGMD. However, as discussed above, many motor behaviours in invertebrates are controlled by ensembles of neurons. The LDCMD has already been postulated to summate with the DCMD (Gray et al., 2010); these other neurons, and as-yet unidentified neurons, are likely to work in tandem as well, with impacts on the locust flight system that have been largely ignored.

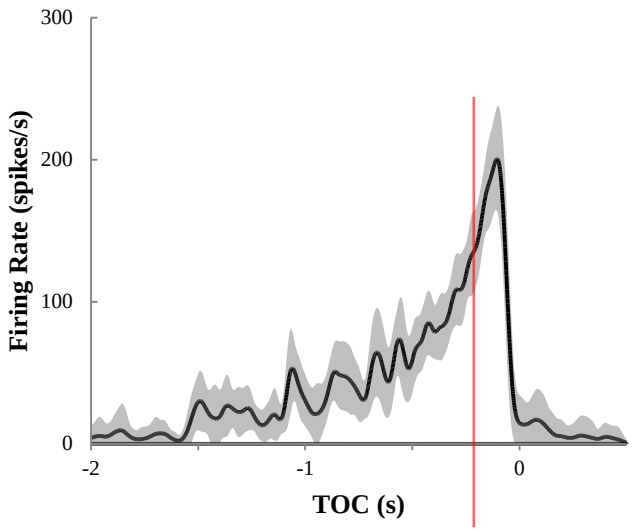

Figure 1.7: Peri-event histogram showing DCMD activity during a looming stimulus. The red line indicates the time of collision. The grey shade represents standard deviation, while the black line indicates the average of twenty animals. Data shown from Chapter 2.

1.5 Stimulus Design

Natural stimuli are complex, presenting a major difficulty in the analysis of a stimulus-response relationship (Felsen and Dan, 2005). Simple artificial stimuli have the advantage that they can be easily controlled and correlated with neuronal responses (Felsen and Dan, 2005). Studies that examine looming detection in locusts predominantly use simple, computer-generated stimuli which include the aspects that are thought to be biologically relevant (Robertson and Johnson, 1993b; Gray et al., 2001; Santer et al., 2006; Rind et al., 2008). Computer rendered objects stimulate the DCMD in the same manner as real looming objects and produce collision avoidance behaviours in tethered flying locusts (Gray et al., 2001). Parameters such as the subtense angle, angular velocity, edge velocity, angular acceleration, and time of collision can be easily manipulated using computer-generated stimuli.

The objects used in this study were scaled to real world coordinates, and the size, shape, and velocities have been shown to produce behaviourally relevant reactions from locusts (Gray et al., 2010; McMillan and Gray, 2012). If avoidance can be effected in the duration of one wing beat after a reaction has been initiated (McMillan et al., 2013), the minimum time needed from the detection of the obstacle is approximately 115 ms (65 ms for neural processing and 50 ms for the wing beat) (Robertson and Johnson, 1993b). The subtense angle that triggers a collision avoidance response in locusts was found to be constant at 10° for approaching objects of varying sizes and speeds (Robertson and Johnson, 1993b). With this subtense angle and the minimum reaction time of 115 ms, an object approaching at 3 m/s (the flight speed of a locust) would need to be more than 35 cm distant with a diameter greater than 6.2 cm to evoke a successful avoidance response, while at 2 m/s the object would need to be 23 cm distant and have a diameter greater than 4.1 cm. Given that the average wing span of a locust is approximately 11

cm (Robertson and Johnson, 1993b), the pectoral diameter of predatory birds is 5-7 cm (Robertson and Johnson, 1993b), and the spacing between individual locusts in a dense swarm ranges from 30 cm to 9 m (Uvarov, 1977), the use of objects at least 7 cm in diameter and traveling at 2 m/s and 3 m/s is biologically relevant.

1.6 Objectives

The two major objectives outlined in this thesis used a similar experimental setup which can be seen in Figure 1.8. This setup allowed for control of computer generated stimuli and precise quantification of neuronal activity. All methods are discussed in detail in Chapters 2 and 3.

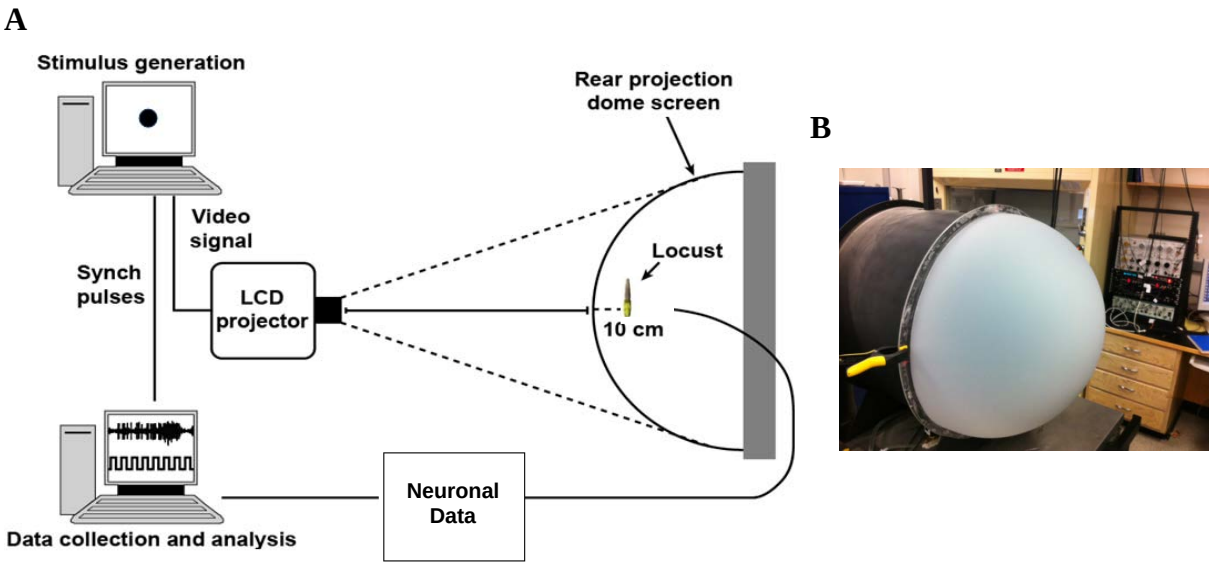

Figure 1.8: General experimental setup for both objectives. (A) Visual stimuli were generated and projected on to a dome-shaped rear projection screen, in which the locust was positioned 10 cm from the apex. Neuronal data was recorded concurrently, digitized, and used to determine neural activity. (B) External image of the rear projection dome.

The visual environment of a flying locust is naturally complex, with objects translating, receding, and looming as a result of their motion in addition to self-motion of the locust itself. The behavioural and neuronal responses of the locust to simple visual stimuli have been well described (Robertson and Johnson, 1993b; Santer et al., 2006; Chan and Gabbiani, 2013), and have recently been expanded to included complex motion (Rind and Simmons, 1992; Guest and Gray, 2006; McMillan and Gray, 2012). These studies strongly suggest that the LGMD/DCMD pathway is capable of encoding, individually, many aspects of visual motion. However, they have yet to be investigated in combination. **Objective 1** of my thesis is to describe the activity of the DCMD in response to visual stimuli, including true translational motion and compound trajectories, in combination with variation in object velocity. Detailed descriptions and results can be found in Chapter 2.

All previous research using *Locusta migratoria* has focused on the activity of individual neurons. At least six visual neurons have been described in the locust, but due to the technological difficulties that led to a focus on the LGMD and DCMD, most have been largely ignored. Furthermore, they have never been recorded concurrently in the same animal. Recent advances, including multichannel electrodes as described above, open the door to investigate these less known neurons simultaneously, in addition to previously undiscovered ones. In **Objective 2**, I investigate the activity of multiple neuronal units in the locust in response to a wide array of visual motion that encompasses most stimuli used in previous experiments. Separated in to two separate sets of experiments, the details and preliminary results are described in Chapter 3.

These experiments are expected to help illuminate the mechanisms that underlie motion-sensitive neurons, including how visual information is coded at the levels of both individual neurons and populations.

CHAPTER 2

[1]SPATIOTEMPORAL STIMULUS PROPERTIES MODULATE RESPONSES TO TRAJECTORY CHANGES IN A LOCUST LOOMING-SENSITIVE PATHWAY*

2.1 ABSTRACT

The Lobula Giant Movement Detector (LGMD) and Descending Contralateral Movement Detector (DCMD) constitute one motion-sensitive pathway in the locust visual system that is implicated in collision-avoidance behaviours. While this pathway is thought to respond preferentially to objects approaching on a direct collision course, emerging studies suggest the firing rate is able to monitor more complicated movements that would occur under natural conditions. While previous studies have compared the response of the DCMD to objects on collision courses that travel at different speeds, velocity has not been manipulated for other simple or compound trajectories. Here we test the possibility that the LGMD/DCMD pathway is capable of encoding complex aspects of object motion including translational motion and trajectory changes at different velocities. We found that the response of the DCMD to translational motion initiated in the caudal visual field was a low amplitude peak in firing rate that occurred before the object crossed 90° azimuth that was invariant to different object velocities. Direct looms at different velocities resulted in peak firing rates that occurred later in time and with greater amplitude for higher velocities. In response to transitions from translational motion to a collision course the firing rate decreased by an amount that was independent of location within the visual field and velocity but with a timing that depended on a combination of

[1] Chapter submitted as a manuscript to the Journal of Neurophysiology

both. These results suggest that this pathway is capable of encoding multiple properties of a moving objects trajectory.

2.2 INTRODUCTION

The natural environment of any animal is a complex combination of sensory stimuli. However, it is adaptive to be vigilant to environmental cues that are salient for a particular animal or species, such as an approaching predator. Rapidly approaching (looming) objects elicit avoidance reactions in many animal species (Gibson, 1958). The behavioural and neuronal responses to looming have been studied in many vertebrate and invertebrate systems, such as crabs (Medan et al., 2007; Oliva and Tomsic, 2012), frogs (Yamamoto et al., 2003), pigeons (Sun and Frost, 1998; Wu et al., 2005), cats (Liu et al., 2011), primates (King and Cowey, 1992; Maier et al., 2004), and humans (Vallis and McFadyen, 2005; Gray and Regan, 2006). Research on looming-sensitive neurons has focused on the mechanisms that underlie responses to objects traveling along simple trajectories, while only recently have the response to complex natural environments been explored (Guest and Gray, 2006; McMillan and Gray, 2012).

Locusta migratoria, the migratory locust, is an ideal system for studying the neural mechanisms that underlie the processing of complex visual motion. Gregarious locusts in a swarm fly as close as 30 cm apart (Uvarov, 1977) with flight speeds of 3-6 m/s (Robertson and Johnson, 1993a), requiring accurate responses to multiple objects traveling at different velocities often along changing trajectories. Behaviourally, an approaching object will evoke a coordinated steering response from a flying locust (Rind and Simmons, 1992; Robertson and Johnson, 1993a; Santer et al., 2006; McMillan and Gray, 2012; Chan and Gabbiani, 2013). The Descending

Contralateral Movement Detector (DCMD) is an identified motion-sensitive neuron in the locust system that, along with its presynaptic partner, the Lobula Giant Movement Detector (LGMD), constitutes one motion-sensitive neural pathway that responds robustly to looming objects (Schlotterer, 1977; Hatsopoulos et al., 1995; Judge and Rind, 1997), but is also sensitive to translating objects within its visual field (Pinter, 1983; Rind, 1987; McMillan and Gray, 2012). The LGMD receives integrated retinal inputs that, during looming, evoke a characteristic increase in firing rate that is transmitted to the DCMD in a 1:1 ratio via a mixed chemical and electrical synapse (Rind, 1984). The firing rate peaks after a defined subtense angle on the retina is exceeded, which occurs near the projected time of collision (Gabbiani et al., 2002; Krapp and Gabbiani, 2005). Subsequently, the DCMD connects to flight interneurons and motorneurons within the thoracic ganglia (Schlotterer, 1977; Simmons, 1980b), implicating this pathway in mediating collision avoidance behaviours (Santer et al., 2006).

Previous experiments have shown that visual information alone can trigger adaptive behavioural responses in locusts (Robertson and Johnson, 1993b; Santer et al., 2006; McMillan and Gray, 2012; Chan and Gabbiani, 2013) and that the DCMD responds to complex scenes (Rind and Simmons, 1992), paired object approaches (Guest and Gray, 2006), objects with compound shapes (Guest and Gray, 2006), and objects following compound trajectories (McMillan and Gray, 2012). These findings strongly suggest that this single pathway may be capable of encoding complex motion, which exists in the locust's natural visual environment. To test this possibility, we presented locusts with the image of a black disk moving with different trajectory parameters (direction, velocity, and course changes). Overall, our findings show that the modulation of the DCMD firing rate reflects aspects of compound visual motion. Stimuli with looming components evoked DCMD responses with characteristic timing and amplitude of

peak firing rate. We found that only the timing of the DCMD responses to non-colliding trajectories was significantly affected by velocity. We also found that DCMD responses to transitions were affected by the velocity of the projected disk as well as the region of the visual field where the transitions occurred. Furthermore, the collision-associated DCMD responses to the looming component of compound trajectories were not affected by the previous translation. These data show that the DCMD remains sensitive to looming after changes in stimulus trajectories.

2.3 MATERIALS AND METHODS

2.3.1 Animals

Gregarious adult male *Locusta migratoria* were obtained from a crowded colony maintained in the Department of Biology at the University of Saskatchewan (25-28°C, 12:12h light-dark cycle). Locusts selected were at least 3 weeks past the imaginal molt. Experiments were carried out at room temperature (~25°C).

2.3.2 Preparation

The experimental setup was similar to that described recently (McMillan and Gray, 2012). The locust's legs were removed and a rigid tether was attached to the ventral surface of the thorax with melted beeswax while the wings were held in place. A small patch of ventral cervical cuticle was removed to expose the underlying paired connectives of the ventral nerve cord anterior to the prothoracic ganglia. The tissue was bathed in a drop of locust saline (in mmol: 147 NaCl, 10 KCl, 4 CaCl2, 3 NaOH, 10 HEPES, pH 7.2), and the preparation was

transferred to the recording stage. Neuronal recordings were obtained from the left ventral nerve connective using two bipolar silver wire hook electrodes insulated with a Vaseline and mineral oil mixture. The preparation was then rotated so that the locust was oriented dorsal side up with the longitudinal axes 10 cm away from and perpendicular to the apex of a rear projection dome screen, so that the right eye was aligned with the azimuthal and elevational axes of the dome apex (see Fig. 1 of Guest and Gray, 2006). In this way, azimuthal positions along the equator of the dome at 0°, 90°, and 180° were directed to the frontal, lateral, and caudal eye equator. The preparation was left for ~15 min in front of a projected white visual field (background luminance = 430 cd/m^2) before presentation of stimuli to allow acclimation to the experimental setup. To prevent confounding effects of neural habituation, the interval between each presentation was at least 3 minutes.

2.3.3 Visual Stimuli

The procedure used for visual stimulus generation and data acquisition was similar to that used by (Guest and Gray, 2006). Visual stimuli were created with Vision Egg visual stimulus generation software (Straw, 2008) on a Python programming platform and represented as 1,024 x 1,024 pixel portable network graphics (png) files. Individual pixel sizes on the projection screen were ~0.7 mm, a visual subtense angle of ~0.4°, below the highest spatial resolution of the compound eye (Horridge, 1978). A 7-cm black disk traveling at five different velocities was scaled in real time at 85 frames/s and projected onto a specialized rear projection dome screen with an InFocus DepthQ LCD data projector, with correction factors embedded in the Vision Egg code to account for the distortion due to projection onto the curved surface of the screen. A 1.2-ms TTL pulse included in each video frame and the vertical refresh synchronization pulse

(vsync) from the video card (NVIDIA GeForce4 Ti4200 128 MB) were used to align physiological recordings with events associated with the stimuli (see below). The last TTL pulse was used to determine the final frame of each presentation, which indicated when the object had disappeared from the screen. The corresponding vsync pulse determined the start time of the rendering of the frame. The luminance values and Michelson contrast ratio (0.48) were the same as those used previously (Guest and Gray, 2006; McMillan and Gray, 2012).

Locusts (n = 20) were presented with a randomized set of visual stimuli while neuronal responses were recorded. All visual stimuli were presented at 0° elevation and position varied only within the azimuthal plane. The stimulus set consisted of five unique trajectories repeated with five different object velocities (Fig. 2.1). Each presentation sequence began and ended with a direct loom from 90° to test for potential hysteresis effects of the duration of the experiment on DCMD responses. All other trajectories were presented in a different random order for each locust. For each presentation the disk remained on the screen for 1 s before disappearing within 1 frame. Direct looms ended 10 cm from the eye of the locust. Trajectory changes occurred over 1 frame.

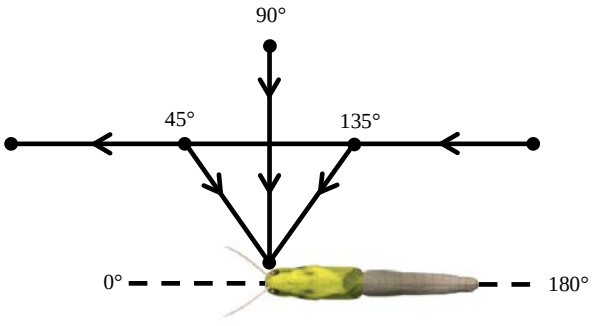

Figure 2.1: Stimulus design. Black disks (7 cm) moved along trajectories that were looming, translating, or transitioned from translating to looming. We presented one simple looming trajectory at an azimuthal angle of 90° that started 400 cm from the locust's eye and one simple translating trajectory that started in the posterior visual field and travelled through 168° (6° to 174°) with a minimum distance from the locust eye of 80 cm. Three compound trajectories were also used, which began translating from the posterior visual field and transitioned to looming at 135°, 90°, or 45° azimuth. All trajectories were repeated for 5 different $l/|v|$ values (10 ms, 20 ms, 30 ms, 40 ms and 50 ms), for a total of 25 unique visual stimuli.

This experiment was designed to test DCMD responses to visual motion that translates before changing to a collision course while travelling at different velocities. We define translation as local small-field motion along a straight trajectory parallel to the longitudinal axis of the locust (Fig. 2.1). This type of translational motion is thus distinct from wide-field optic flow induced during translatory self-motion of the animal and small-field motion within the azimuthal plane at a fixed distance from the animal. Here we used a minimum distance of 80 cm (a subtense angle of 5° at 90° azimuth) for translational motion, an intermediate distance shown to evoke robust DCMD responses (McMillan and Gray, 2012). Disks that followed trajectories with no translational component approached from 400 cm at 90° azimuth. Trajectories with no looming component travelled across 168° of the azimuthal plane (6° to 174°).

To test the effects of trajectory changes during object motion, we presented compound trajectories that contained translatory and looming components. For all compound trajectories, motion began in the posterior visual field and traveled along a translatory trajectory as described above. Translatory motion transitioned to looming at 45°, 90°, or 135° azimuth.

To test the effect of velocity, we presented each trajectory type (looming only, translating only, and three compound trajectories) at five different speeds. We calculated the ratio of the object half size (l) and absolute velocity ($|v|$), which characterizes the stimulus profile during looming (Gabbiani et al., 1999). Though translating objects did not loom, for consistency in data presentation we assigned $l/|v|$ values that matched the velocity of looming discs. The size of the projected disc was constant for all trajectories (7-cm diameter), and therefore velocity was varied to produce different $l/|v|$ values (smaller $l/|v|$ represented a faster approach). We used $l/|v|$ values distributed evenly between 10 and 50 ms (Gabbiani et al., 2002), which are biologically relevant (Santer et al., 2012).

2.3.4 Spike Sorting and Quantification of DCMD Firing Properties

For each stimulus presentation we recorded continuously and stored neuronal activity from the left cervical connective, pulses synchronized with each frame of the stimulus, and vsync pulses from the video card for analysis. Recorded neural activity was amplified with a differential AC amplifier (A-M Systems, model no. 1700, gain = 10,000) and sampled at 25 kHz. An RP2.1 enhanced real-time processor (Tucker-Davis Technologies, Alachua, FL) with Butterworth filter settings of 100 Hz (high pass) and 5 kHz (low pass) was used to store the data to disk. The characteristically large amplitude DCMD spikes were identified by threshold analysis in Offline Sorter (Plexon, Dallas, TX). Spike times were exported to Neuroexplorer analysis software (NEX Technologies, Littleton, MA), and spike times were transformed into peristimulus time histograms with a l ms bin width and smoothed with a 50 ms Gaussian filter (Fig. 2.2). To characterize DCMD firing properties we measured the firing rate (f) for each local peak or valley in firing rate as well as the peak width at one-half the maximum firing rate for TOC-associated peaks. We also measured response delays (δ) from time of transition (TOT), time of collision (TOC) or time that the object crossed 90° azimuth (T90). Linear regressions of $l/|v|$ values and response parameters were used to calculate the slope (m) and y-intercept (b) of the relationships.

In previous work that presented compound trajectories (McMillan and Gray, 2012) the change in firing rate (f') and expansion characteristics of the visual stimuli were used to develop a two-dimensional (2D) Gaussian model. Our data, with additional manipulation of object velocity, were used to further test the validity of the model. Briefly, the instantaneous angular acceleration of the subtense angle (θ'') and the instantaneous azimuthal angular acceleration of the leading edge (ψ'') of the projected disks were calculated over the transition from translational

to looming motion. Current and previous results were fit with the 2D Gaussian equation used by (McMillan and Gray, 2012).

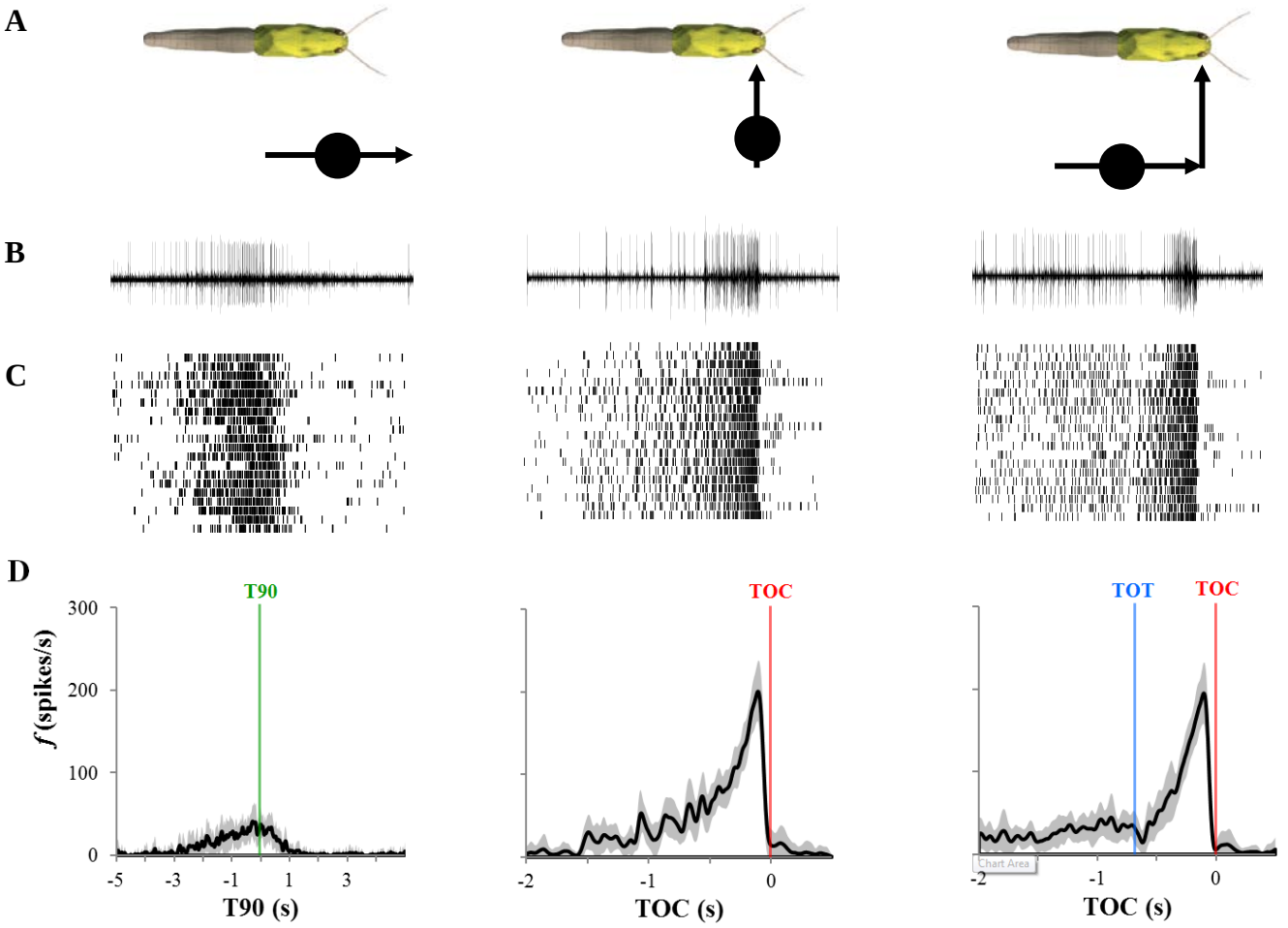

Figure 2.2: DCMD responses to three different trajectories with $l/|v|$ values of 30 ms. (A) Diagrams of trajectories. (B) Raw neuronal recordings from one animal showing DCMD activity. (C) Raster plots from 20 different animals showing DCMD spikes over stimulus presentation. (D) Peristimulus time histogram showing the average firing rate from 20 animals (black) with standard deviation (grey shade). Translating objects evoked a relatively low peak in firing rate at the time the object crossed 90°. Looming stimuli evoked a characteristic increase in the firing rate with a peak approximately 100 ms before TOC. Transitioning to looming evoked a decrease in the firing rate within 200 ms following TOT, followed by a characteristic looming response.

2.3.5 Statistical Analysis

DCMD firing parameters were tested for putative effects of velocity and direction with SigmaStat 3.5 and plotted with SigmaPlot 10.0 (Systat Software, Richmond, CA). Parametric data were tested with a one-way ANOVA and plotted as line graphs with means ± standard deviation (SD), whereas nonparametric data were tested with a Kruskal-Wallis ANOVA on ranks and plotted as line graphs with means ± SD. Tukey's or Dunn's post-hoc test were used as appropriate. Strength of linear dependence between firing parameters and velocity were measured with Pearson product-moment correlation coefficients (PCC). All significance was assessed at $p < 0.05$.

2.4 RESULTS

2.4.1 Translation

Translating disks evoked slow increases in DCMD spike rate, with a low amplitude peak near T90, followed by a decrease to resting firing rate (Figs. 2.2 and 2.3). While there were no significant difference between $l/|v|$ values, we found a weak correlation between the $l/|v|$ and the timing of the peak (r = -0.21; Fig. 2.4A).

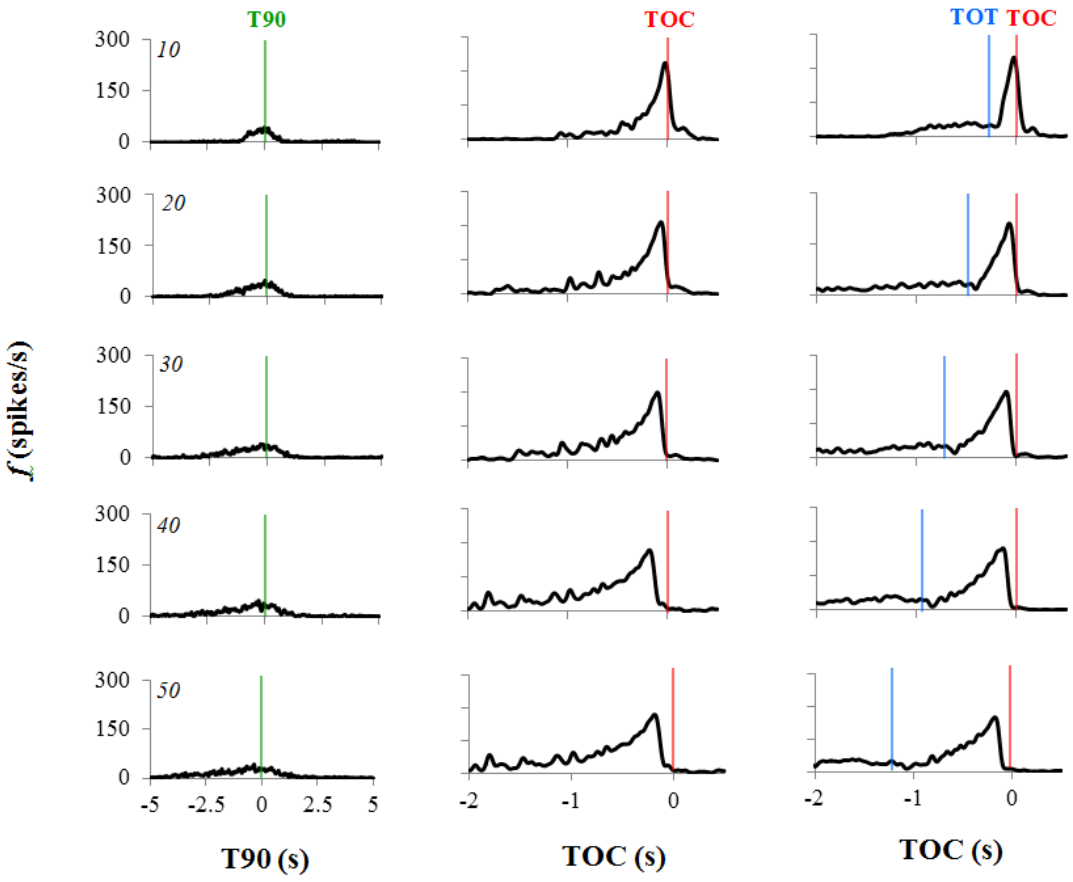

Figure 2.3: Response profiles (time histograms) for five $l/|v|$ values and three trajectories showing the average DCMD response (n = 20). $l/|v|$ values are indicated in the leftmost panel. The time range for translating stimuli was increased to encompass the entire stimulus presentation. Green bars indicate T90, red bars indicate TOC, and blue bars indicate TOT. For all looming components, objects approached at 90°. The low amplitude peaks in response to translating stimuli occurred earlier with increased $l/|v|$. For looming stimuli, higher $l/|v|$ values produced lower amplitude, wider, and earlier peaks in firing rates. For all $l/|v|$ values, transition to looming evoked a clear valley which was followed by a characteristic increase in firing rate during the looming component of the approach.

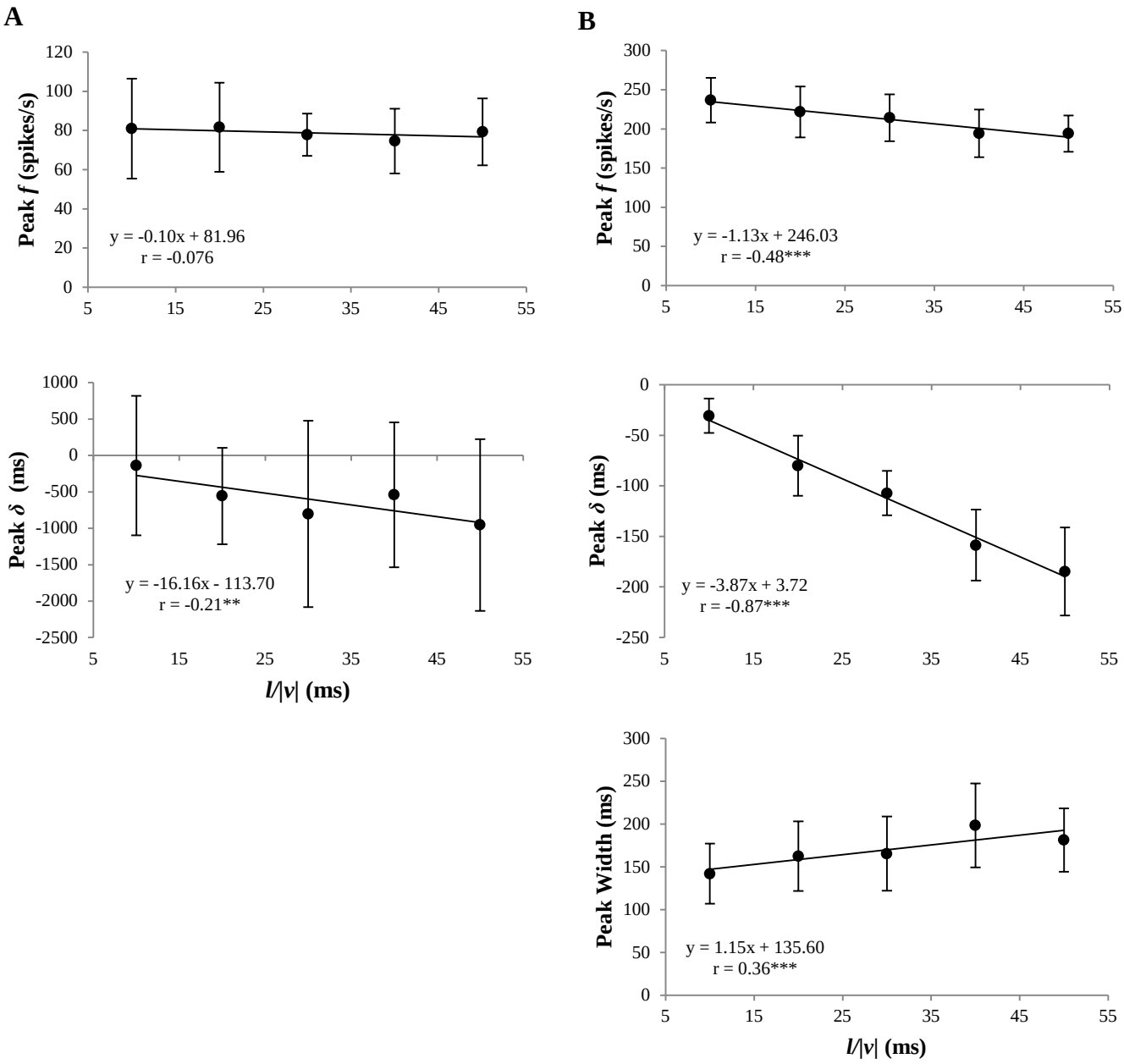

Figure 2.4: Parameters of the DCMD response to translating (A) and looming (B) trajectories. Mean peak firing rate and time with standard deviation (n=20) for five different $l/|v|$ values are shown for both translating and looming stimuli, with the addition of peak width for responses to looming. Peak times are relative to T90 (translating) or TOC (looming). Equation of the line and PCC are given for each. (A) Translating stimuli evoked earlier peaks with higher $l/|v|$ values, but had no significant difference in peak amplitude. (B) Peaks in the firing rate occurred earlier and were lower and wider for looming stimuli with higher $l/|v|$ values.

2.4.2 Looming

Looming disks evoked consistent and characteristic DCMD responses with a spike rate that increased during object approach and peaked near TOC (Figs. 2.2 and 2.3). Comparing data from the first and final approaches at 90°, we found no significant differences in the peak firing amplitude, peak time, or peak width at half-maximum amplitude (data not shown). Therefore, there was no hysteresis effect on the duration of each experiment.

The $l/|v|$ value of the projected disk significantly affected the peak firing rate (H_4 = 26.36), peak time (H_4 = 79.56), and peak width at half-maximum (F_4 = 5.00, Fig. 2.4B. Furthermore, the $l/|v|$ value was significant correlated with peak firing rate (r = -0.48), peak time (r = -0.87) and peak width at half-maximum height (r = 0.36).

2.4.3 Compound Trajectories

Disks following trajectories that transitioned from translational motion to looming evoked a DCMD response with a TOT-associated decrease in firing rate and a subsequent increase in firing rate leading to a TOC associated peak (Fig. 2.5). The translatory component of the trajectory evoked a slow increase in firing rate as the disk approached 90° azimuth. For trajectories where the disk passed through 90°, the firing rate decreased again as the object continued translation.

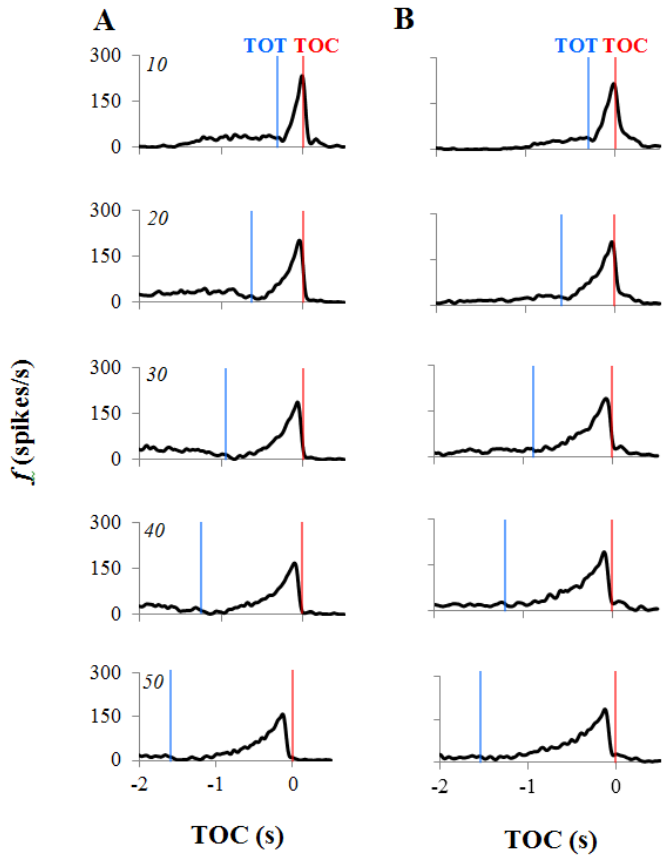

Figure 2.5: Response profiles for the average DCMD response (n = 20) to visual stimuli transitioning between translation and looming at 45° (A) or 135° (B) azimuth with five different $l/|v|$ values (indicated in leftmost panel). Transitions to both approach angles valleys that were most distinct for lower $l/|v|$ values (10 and 20 ms). (A) For $l/|v|$ values of 30 to 50, the response is similar to responses to pure translation, with the firing rate decreasing almost to a resting value after the disk crossed 90° azimuth. (B) The translational component has little effect on the firing rate for higher $l/|v|$ values.

2.4.4 Velocity

For transitioning stimuli the $l/|v|$ value significantly affected the valley amplitude (H_4: 135° = 48.94, 90° = 33.38, 45° = 64.76) and peak time (H_4: 135° = 77.89, 90° = 80.12, 45° = 89.07) at all transition angles. Valley times were also affected for transitions at 135° and 90° (H_4: 135° = 18.04, 90° = 31.36), but not for transitions at 45° (H_4 = 35.45). The peak was

significantly wider for higher $l/|v|$ values (H_4: 135° = 10.28, 90° = 21.86, 45° = 31.68), and the firing rate at TOT was lower for 135° (H_4 = 34.68) and 45° approaches (F_4 = 2.89). We found significant correlations between $l/|v|$ and all parameters except for the firing rate at TOT for compound trajectories with 90° looms, the difference in firing rate between TOT and the valley for 135° and 45° looms, and the timing of the valley for 45° looms (Fig. 2.6).

2.4.5 Approach Angle and Velocity

With respect to $l/|v|$ values, the timing of the TOC-associated peak for compound trajectories at approach angles of 45° followed trends with greater y-intercepts than 90° (q = 6.72) and 135° approaches (q = 6.01), and with a slope greater than 135° approaches (q = 8.45), which itself had a lower slope than 90° transitions (q = 9.84). The regression between primary peak width and $l/|v|$ had a greater y-intercept for 45° approaches than 135° (q = 3.71). The slope of the trend for firing rate at TOT versus $l/|v|$ was less for 90° approaches than 135° (q = 3.57), while the slope for the difference in firing rate between TOT and valley was greater for 90° than for 45° (q = 3.64). For valley time, trajectories that transitioned at 45° had lower y-intercepts than 90° (q = 7.71) and 135° transitions (q = 7.04), but greater slopes than 90° (q = 5.43) or 135° (q = 7.36). No other significant differences were found between the trends of parameters and $l/|v|$ value. In summary, the response of the DCMD to compound trajectories was dependent on both $l/|v|$ value and transition angle for the timing and width of the TOC-associated peak, the firing rate at TOT, and the difference between TOT and valley firing rate, and the timing of the valley.

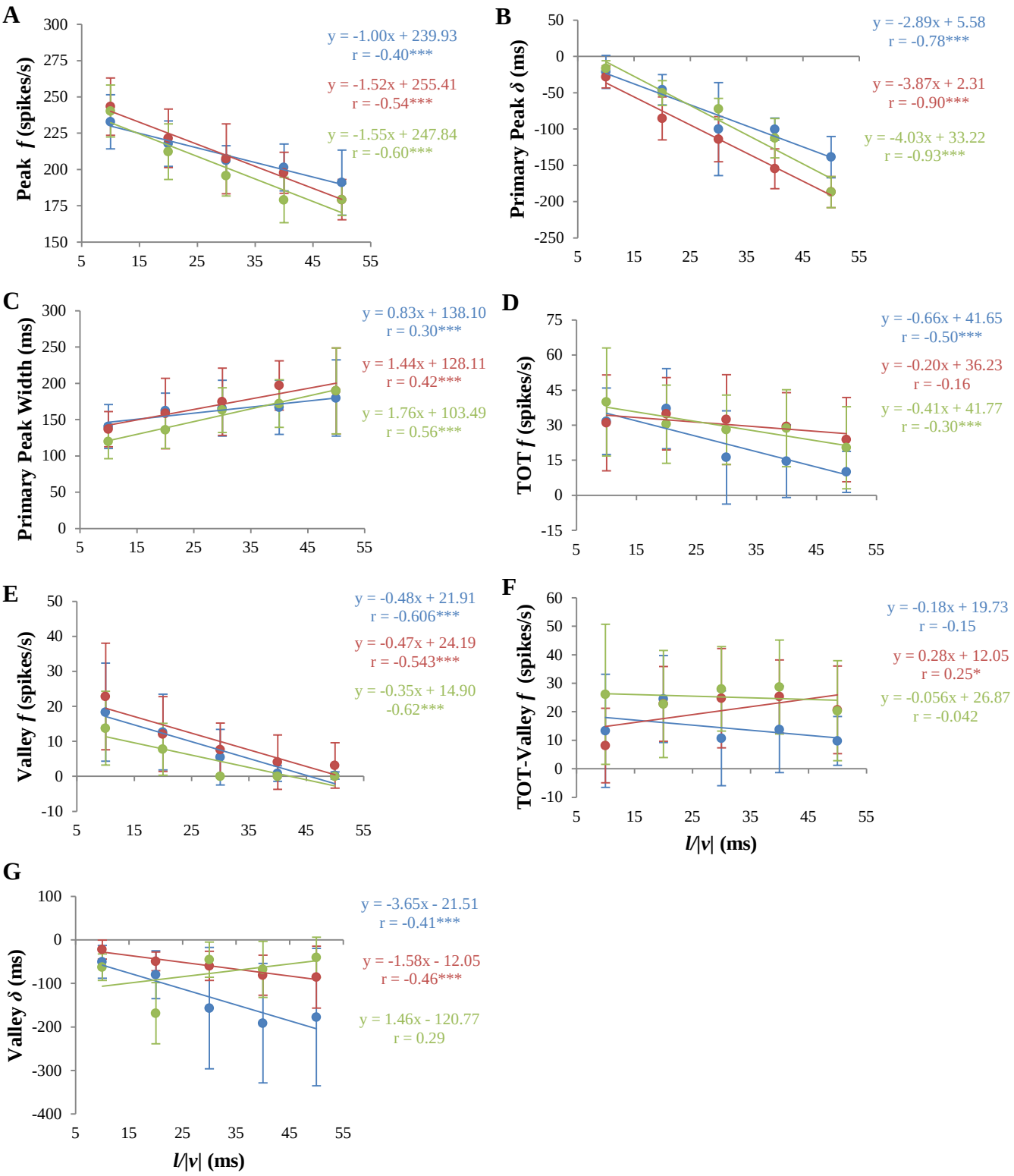

Figure 2.6: (A-G) Comparison of DCMD firing parameters between responses to compound trajectories with three different angles of approach (blue: 135°, red: 90°, green: 45°) for five $l/|v|$ values. Mean with standard deviation (n = 20) are given. Linear regression and PCC are given for each. The relationship between $l/|v|$ value and parameter are not significantly different between transition angles except for firing rate at TOT (D), TOT-Valley firing rate (F), and valley timing (G). All correlations are significant except for the valley timing for 45° approaches, firing rate at TOT for 90° approaches, and TOT-Valley firing rate for 135° and 45°.

2.4.6 Expansion Properties at Trajectory Changes

Previous experiments have described the expansion properties of objects following trajectories that transition between translating and looming that differed with respect to trajectory prior to transition, the proximity of the transition, and the time of transition within stimulus presentation. We combined out data here with those of (McMillan and Gray, 2012) and fit them with the 2D Gaussian equation as they described;

$$f' = 2.9e^{-0.5\left[\left(\frac{\theta'' + 10.1}{-26.9}\right)^2 + \left(\frac{\psi'' + 169.8}{211.6}\right)^2\right]}$$

The amplitude change (f') was predicted by θ" and ψ" ($r^2 = 0.56$) whereas the response time (δ) was poorly fit ($r^2 = 0.18$, Fig. 2.7). These data suggest that modulation of the DCMD firing rate was related to the unique trajectory changes of a moving object, while the response time was invariant.

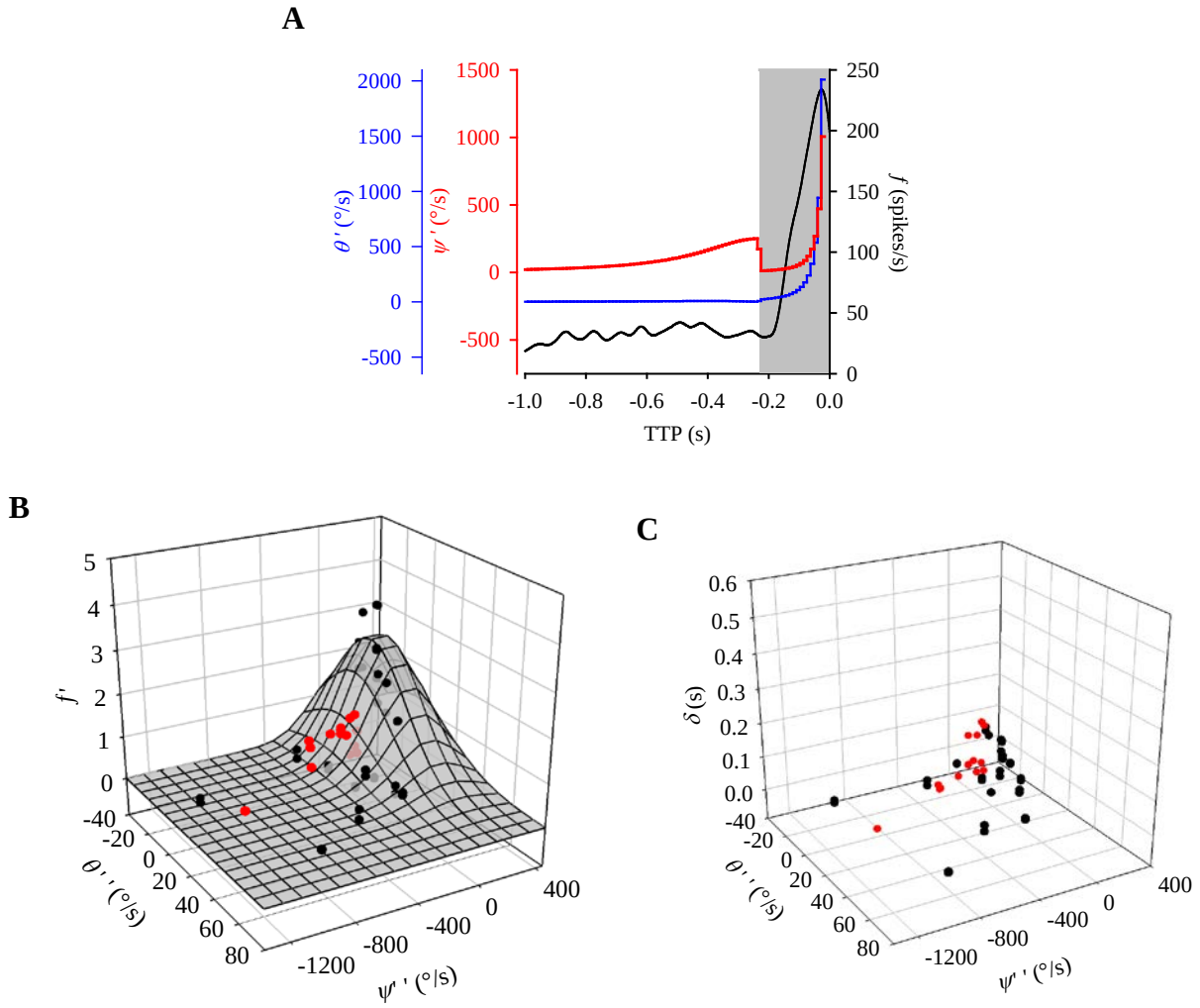

Figure 2.7: Correlation of DCMD firing modulation with expansion parameters during trajectory transitions. (A) Sample data from presentation of a 7-cm disk travelling along a compound trajectory consisting of translation from the posterior with a transition to looming at 90° with an $l/|v|$ of 30 ms. The subtense angular velocity (θ', blue line) and rotational velocity of the leading edge of the disk (ψ', red line) changed abruptly at the trajectory change and preceded modulation of the DCMD firing rate (f, black line). The gray shaded area indicates a looming trajectory with the margin at TOT. (B) Current (red) data from the mean firing rate change (f') at the time of transition were plotted against the subtense angular acceleration (θ") and the rotational acceleration of the leading edge (ψ") with previous data (black; McMillan and Gray 2012). The resulting scatterplot was fit with a Gaussian equation (gray mesh). (C) Data for the mean response time did not satisfy the tolerance of a Gaussian equation. Axes were scaled according to the range of values for each variable.

2.5 DISCUSSION

This is the first study to quantify and compare the firing of a locust visual interneuron to objects that transition from translation to looming while travelling at different velocities. DCMD responses to objects looming with different $l/|v|$ values were consistent with previous findings showing that high $l/|v|$ values evoked lower, wider, and earlier peaks in the firing rate. We found that in response to translation, the DCMD peak firing rate was invariant to different $l/|v|$ values and only weak correlations showing earlier peaks with higher velocities. As the $l/|v|$ value is a ratio of the object size and velocity, these data suggest that the DCMD does not encode unique properties an object's translational velocity. We also found that the DCMD firing rate was modulated in a trajectory and velocity dependent manner for transitions to looming. This suggests that the DCMD is able to encode both the object velocity and trajectory, and may reflect perceived threat. Finally, we support the previously proposed relationship between change in firing rate and unique expansion properties (θ'' and ψ'), with invariant response time (McMillan and Gray, 2012).

2.5.1 Looming

The DCMD response to a looming disk was a stereotyped increase in firing rate with a peak just before TOC (Fig. 2.2), which is consistent with previous reports (Rind and Simmons, 1992; Gabbiani et al., 1999; Gray et al., 2001; Gray, 2005; McMillan and Gray, 2012). While the $l/|v|$-dependent peak firing rate and time resemble findings from Gabbiani et al. (2002), there is some discrepancy. For example, we report much higher peak firing rates that decayed more slowly with an increase in $l/|v|$ values. (Rind and Santer, 2004) attribute the low firing frequency

to postsynaptic feed-forward inhibition (Rind and Bramwell, 1996) caused by the exaggerated size of the visual stimuli used (a 40 ms $l/|v|$ square was 16 cm x 16 cm and approached at 200 cm/s, while a similar $l/|v|$ here corresponds to a 7 cm diameter disk approaching at 87.5 cm/s). Conversely, Rind and Santer (Rind and Santer, 2004) propose that the firing rate of the LGMD and thus the DCMD should increase until after the time of collision, which does not coincide with our results. Peak widths found here were intermediate to previous results, with results higher than McMillan and Gray (McMillan and Gray, 2012), which used low $l/|v|$ values, but lower than (Gray et al., 2010), which used higher $l/|v|$ values.

2.5.2 Translating

While the LGMD/DCMD pathway responds vigorously to looming objects (Schlotterer, 1977; Gabbiani et al., 1999; Krapp and Gabbiani, 2005), it also responds to small, translating objects (Palka, 1967; Pinter et al., 1982; Peron and Gabbiani, 2009b; McMillan and Gray, 2012). Consistent with previous reports (McMillan and Gray, 2012), the projected translating disks evoked an increase in the DCMD firing rate, with a peak near the time the object crossed 90° azimuth. We found weak negative correlations between the $l/|v|$ of the translating disk and the timing of the peak in firing rate, such that the peak occurred earlier in time for larger $l/|v|$ values (Fig. 2.3A). This is the first experiment to directly examine the effect of translational velocity on response of the locust DCMD. Previous studies either used stimuli which differed from the translatory motion defined here (Peron and Gabbiani, 2009b) or did not manipulate object velocity. True translation in three-dimensional space would contain a looming component (see

(McMillan and Gray, 2012), which is supported by the earlier peak found with higher $l/|v|$ values, as shown here (Fig. 2.4).

2.5.3 Trajectory Changes and Object Velocity

Transition from translation to looming affects the expansion properties of a disk in a manner dependent on the distance and type of trajectory change (McMillan and Gray, 2012). Our data show that the change in expansion properties is also affected by the velocity of the disk. At a transition from translation to looming, the instantaneous subtense acceleration (θ'') increased while the acceleration of the leading edge (ψ'') decreased, coinciding with a decrease in the DCMD firing rate (Fig. 2.7A). In combination with data from (McMillan and Gray, 2012), we found that f' was correlated with θ'' and ψ'' ($r^2 = 0.56$), while the timing of the response was invariant ($r^2 = 0.18$). Although these data support the previously reported correlation for a wider range of stimuli, the underlying biophysical mechanism remains to be determined.

While our data show that the TOC-associated peak in DCMD firing rate was not affected by the initial translational motion, it does show location-dependent modification of TOT-associated features of the DCMD response (Fig. 2.6). The velocity-driven modulation of firing rate, peak time, and peak width of the TOC-associated peak was invariant of approach angle. However, the firing rate at the TOT and the time between the TOT and the associated valley responded to velocity changes in a manner that was dependent on the location of the transition within the locusts' visual field. The instantaneous firing rate at TOT for approaches from 45° and 135° decreased for higher $l/|v|$ values and there was no significant effect of $l/|v|$ for 90° looms (Fig. 2.6), while instantaneous firing rate at the TOT associated valley was correlated with $l/|v|$ value

for all angles of approach. However, the difference between firing rate at TOT and at the associated valley was only correlated with $l/|v|$ value for 90° looms and was not significantly different between approach angles. This suggests that the firing rate decreased a fixed amount after the disk began to loom. Moreover, the time from TOT to the valley was independent of $l/|v|$ only for an approach of 45°. These results show that, while the LGMD/DCMD pathway remains sensitive to looming objects, there is velocity and location dependent modulation of the response to trajectory change.

2.5.4 DCMD Responses to Compound Trajectories and Velocity

The currently accepted model of LGMD activity suggests that it is controlled by excitation spreading through retinotopic inputs from the eye (Peron et al., 2009), which is modulated by feedforward inhibition onto a branch of the LGMD (Rind and Bramwell, 1996; Gabbiani et al., 2002). This suggests that the LGMD performs a multiplicative computation resulting in an increase in firing rate during object approach related to $l/|v|$ (Gabbiani et al., 2002). This model also explains how the DCMD is able to respond to novel stimuli after habituation (Gray, 2005) and to multiple object approaches (Guest and Gray, 2006). Our data are also consistent with this model. Translational motion results in an increased firing rate as the object expands with an increase in the velocity of the leading edge (Fig. 2.2 and 2.3). The firing rate decreases when the leading-edge expansion decreases across the ommatidia, either at the point of transition to looming or as the object crosses 90° azimuth. This decrease in expansion would allow feedforward inhibition to counteract excitation in synchrony with a reduction in presynaptic excitation, with additional adaptation at the level of the LGMD membrane (Peron

and Gabbiani, 2009b), ultimately resulting in the observed reduction in firing rate. In the case of a non-colliding trajectory, θ would continue to decrease, allowing inhibition to dominate, causing a decrease in firing rate to the resting level. This can also be used to explain the difference in peak time for translation with different velocities. A slower moving object with identical size will have a lower leading edge velocity, allowing feedforward inhibition greater influence on the firing rate. Concurrently, the slower moving object allows more time for adaptation, resulting in the overall inhibition overcoming the excitation due to expansion more quickly, which is presented as an earlier peak time (Fig. 2.3).

While the response of the LGMD/DCMD pathway to direct looms in different regions of the locusts' visual field was not tested here, previous results have shown that there is no difference in response to looms within a range of 30-150° azimuth (Krapp and Gabbiani, 2005). The data presented here supports these findings for all looming motion. However, components of the LGMD/DCMD response that are associated with transitions appear to show local sensitivity. In particular, the timing of the valley has opposing trends most evident when compared between transitions at 45° and 135° (Fig. 2.6). For transitions in the frontal region of the eye, the decrease in firing rate after TOT reaches its minimum sooner than for transitions in the caudal region. The eye of the locust has an acute zone of maximal ommatidial density in the frontal equatorial region (Horridge, 1978; Krapp and Gabbiani, 2005), but which has a lower sensitivity to motion that is attributed to a greater electrotonic distance from the spike initiation zone of the LGMD, resulting in attenuation of electrical signals (Krapp and Gabbiani, 2005; Peron et al., 2007). The more rapid drop in firing rate could be related to the decrease in ψ'' occurring over a larger subset of ommatidia than at the other two locations used. A simultaneous drop in excitation of many ommatidia, particularly those with the greatest electrotonic distance and thus the most

dependent on synchronized membrane depolarization, could result in a more rapid decrease in firing rate. When coupled with adaptation resulting from a slower-moving stimulus, this would result in the firing rate reaching the minimum more quickly, explaining the observed negative correlation (Fig. 2.6).

McMillan and Gray (2012) suggested that the drop in firing rate after a trajectory change may reset the LGMD/DCMD pathway to a firing rate below that associated with the threshold angle implicated in looming detection (Gabbiani et al., 1999). They also found that the size of the drop was dependent on the distance that the transition occurred relative to the locust. Our data supports that the change in firing rate may reset the system, but found the timing of the change, rather than the magnitude, to be related to both $l/|v|$ and location within the visual field. While there was variation in the firing rate both at TOT and the subsequent valley (Fig. 2.5), there was limited change in the difference between TOT and valley firing rate for any of the angles or $l/|v|$ values tested (Fig. 2.6). This suggests that through a combination of firing rate at TOT, firing rate at the valley, and the timing of the valley, the LGMD/DCMD pathway is capable of encoding object distance, velocity, size, location, and direction at a transition between looming and translation. These data support recent findings that suggest multiplexing of parameters of DCMD firing, shown to be implicated in visually triggered escape jumps (Fotowat et al., 2011). The instantaneous firing rate change may encode the presence of a trajectory change while the firing rate over the subsequent tens of milliseconds encodes the additional, behaviourally relevant, information. In addition, while previous studies suggest that escape behaviours are triggered by activity exceeding a threshold (Santer et al., 2006; Fotowat and Gabbiani, 2007), another motion-sensitive neuron with coincident firing has been identified in the locust system (Gray et al., 2010). This presents the possibility that the activity of other visual

neurons may compound the observed responses of the DCMD, potentially including the response to transitions in trajectory. However, further investigation of the DCMD and other visual neurons to the stimuli used here is necessary.

Our suggestion that the locust LGMD/DCMD pathway is capable of encoding aspects of complex object motion is supported by findings in other systems. Lobula plate tangential cells in the hoverfly *Eristalis* are capable of coding directionality of both elementary and figure motion (Lee and Nordström, 2012). Dragonflies use small target motion detector neurons to track prey targets, with individual neurons that are selective to targets even within clutter (Nordstrom et al., 2006) and other neurons that are active on a longer time scale, thought to enhance overall sensitivity of the system (Dunbier et al., 2012). In primates, neurons in the medial superior temporal area of the visual cortex respond to expansion, rotation, and deformation to control important behavioural functions (Mineault et al., 2012). It is important to note that while many individual neurons in these systems show the capability to encode complex motion, they always work in conjunction with other neurons within their system. To this end, future experiments with the locust system will investigate other motion-sensitive neurons, both individually and as a population. In addition, wind tunnel experiments using similar stimuli to that used here are necessary to correctly correlate neuronal and behavioural responses.

CHAPTER 3

NOVEL INTERNEURONS IN THE LOCUST CONNECTIVE RESPOND TO SIMPLE AND COMPLEX VISUAL MOTION

3.1 ABSTRACT

The migratory locust (*Locusta migratoria*) has been used extensively as a model in neuroethology, particularly for its robust visual system and collision-avoidance behaviours. The vast majority of previous research has focussed on a single motion-sensitive pathway, made up of the Lobula Giant Movement Detector (LGMD) and the Descending Contralateral Movement Detector (DCMD). This pathway has been well described, and is implicated in producing escape behaviours in response to objects approaching on a direct collision course. Recent findings suggest that it is also capable of encoding complex sensory information related to object motion. However, these are not the only visual neurons in the locust system. At least five additional visually-sensitive interneurons have been described, with most first characterized over 25 years ago. Due to the tractability of the DCMD, these neurons have been largely ignored. With modern advancements in multichannel recordings and spike sorting algorithms, it is now possible to re-evaluate the activity of these neglected neurons. To this end, we recorded from the connective of *Locusta migratoria* with multichannel electrodes while presenting a range of visual stimuli including translation, looming, receding, and transitions in trajectories. Together, these stimuli encompass the majority of stimuli used historically and recently for study of the DCMD. We found evidence of multiple neuronal units with responses to visual motion that are both novel

and unique. These findings suggest that visually-evoked behaviours in the locust are controlled by an ensemble of visual neurons, rather than one principal pathway.

3.2 INTRODUCTION

The visual environment of any animal is complex. The abundance, potentially over-abundance, of information is a burden on any system. However, in response to natural selection, many animals have evolved systems that take advantage of only the salient features of sensory inputs (Zupanc, 2010). In the migratory locust, the Lobula Giant Movement Detector (LGMD) and Descending Contralateral Movement Detector (DCMD) form a single pathway that integrates the locusts' entire field of view (Rowell, 1971). This pathway, the most thoroughly characterized in the locust system (Fotowat and Gabbiani, 2011), is implicated in the production of collision avoidance behaviours (Santer et al., 2006), a response that is critical for the survival of the animal. However, it is unlikely that the LGMD and DCMD are the only neurons involved in these behaviours.

Motor systems in invertebrates and vertebrates are often controlled by populations of neurons working in an ensemble, such as in the lamprey (Dubuc et al., 2008), the crab (Hedrich et al., 2011), and the dragonfly (Gonzalez-Bellido et al., 2013). Furthermore, parallel visual pathways that evoke escape behaviours have been reported in *Drosophila* (Fotowat et al., 2009) and fish species (Eaton et al., 2001). In the locust connective at least five visually-sensitive neurons other than the DCMD have been identified. The Descending Ipsilateral Movement Detector (DIMD) is one such neuron, with an axon that runs from inputs at the eye to the flight motor neurons in the thoracic ganglia through the ipsilateral nerve cord, i.e. opposite the DCMD (Rowell, 1971; Burrows and Rowell, 1973). With responses to approaching, or looming, objects

that are almost indistinguishable to that of the DCMD (Fotowat et al., 2009), the DIMD is thought to provide redundancy, protecting a crucial behaviour (Santer et al., 2008). Moreover, it appears to summate with the DCMD (Rowell, 1971; Burrows and Rowell, 1973), a mechanism which has been suggested for another recently identified neuron, the late DCMD (LDCMD; (Gray et al., 2010). The LDCMD appears to encode distinct properties of visual stimuli, with response parameters different from the DCMD and weaker habituation to repeated approaches in the same region of the visual field (Gray et al., 2010). Three other identified neurons, the Ipsi-, Medial, and Contralateral Deviation-Detector Neurons (DNI, DNM and DNC, respectively)((Griss and Rowell, 1986), respond to large field visual motion with dependence on velocity, amplitude, and directionality (Rowell and Reichert, 1986). None of these neurons have been investigated other than with the most simple visual stimuli, and never within the same animal.

To this end, we recorded from the connective of *Locusta migratoria* using multichannel electrodes while presenting a wide variety of visual stimuli. These preliminary findings show the presence of multiple motion-sensitive neuronal units, including those with response characteristics similar to those of the DCMD and LDCMD. Other unidentified units that responded to visual motion were found, but at much lower frequency. These data suggest the presence of currently undescribed populations of neurons in the locust visual system, with potential inter-neuronal activity.

3.3 MATERIALS AND METHODS

3.3.1 Animals

Gregarious adult male locusts (*Locusta migratoria*) were obtained from the crowded colony maintained at the University of Saskatchewan in the Department of Biology, kept at 25-28°C with a 12 hour light-dark cycle. Locusts were selected at no less than 3 weeks past the imaginal molt, and experiments were carried out at room temperature (~25°C).

3.3.2 Preparation

Following restraint of the wings and removal of the legs, a rigid tether was attached to the ventral surface of the thorax with melted beeswax. A square of anterior thoracic cuticle was removed using a sapphire blade to expose the paired connectives of the ventral nerve cord between the suboesophageal and prothoracic ganglia. Following removal of fat bodies and other occluding tissues, the translucent protective sheath surrounding either the right (Experiment 1) or left (Experiment 2) connective was carefully cut using the sapphire blade and removed using fine forceps. The tissue was bathed in a drop of locust saline (in mmol: 147 NaCl, 10 KCl, 4 $CaCl_2$, 3 NaOH, 10 HEPES, pH 7.2) and the preparation was transferred to the recording stage. Following insertion of a silver ground wire in to the abdomen, a multichannel electrode with 2x2 tetrode array of 16 channels (NeuroNexus Technologies, MI, USA) was carefully inserted in to the desheathed connective and maneuvered until a high quality recording was achieved on at least four recording sites. The entire preparation was then rotated so that the locust was oriented dorsal side up, either perpendicular (Experiment 1) or parallel (Experiment 2) to the dome, with the

head aligned at the azimuthal and elevational axes. Azimuthal positions were dependent on experiment; the apex of the dome was 0° relative to the locust for Experiment 1 and 90° for Experiment 2. The preparation was left for ~15 min in front of a projected white visual field (background luminance = 430 cd/m^2) before presentation of stimuli to allow acclimation to the experimental setup. To prevent confounding effects of neural habituation, the interval between each presentation was at least 3 minutes.

3.3.3 Visual stimuli

The procedure for generation of visual stimuli was similar to that used by (Guest and Gray, 2006). Vision Egg software (Straw, 2008) running on a Python programming platform created visual stimuli as 1,024 x 1,024 pixel portable network graphics (png) files. Individual projected pixels were ~0.7 mm, a visual subtense angle of ~0.4° and below the highest spatial resolution of the locust compound eye (Horridge, 1978). Stimuli were projected onto a specialized rear projection dome screen with an InFocus DepthQ LCD data projector at either 60 (Experiment 1) or 85 (Experiment 2) frames/s. Correction factors embedded in the Vision Egg code accounted for distortion due to projection onto the curved surface. A 1.2-ms TTL pulse included in each video frame and the vertical refresh synchronization pulse (vsync) from the video card (NVIDIA GeForce4 Ti4200 128 MB) were used to align physiological recordings with the stimuli. The last TTL pulse was used to determine the final frame of the presentation, indicating the disappearance of the object from the screen. The corresponding vsync pulse thus determined the start of frame rendering. All visual stimuli involved the movement of a 7 cm diameter black disk along predesigned trajectories. The luminance values and Michelson contrast ratio (0.48) have been used previously (Guest and Gray, 2006).

3.3.3.1 Experiment 1: Velocity and trajectory

This experiment was designed to investigate the response of multiple neurons to simple stimuli with different types of motion (looming, receding, translating), velocity, and location within the visual field. Velocity was described by the $l/|v|$ value, a ratio of the objects half size (l) and absolute velocity ($|v|$), which characterizes the stimulus profile during looming (Gabbiani et al., 1999). For the purpose of consistency, the $l/|v|$ value was also used to describe non-looming trajectories. Locusts (n = 22) were presented with 14 stimuli: six frontal (0° azimuth) looms with $l/|v|$ values of 5.5. 10.8, 21.5, 32.5, 43.2, and 53.8 ms, looms with $l/|v|$ values of 10.8 ms at 45° azimuth from either side, 67.5° to the right, 45.5° from above and below, receding at 0° azimuth, and translation 20 cm distant through 154.4° and 165.7° with $l/|v|$ values of 40 ms (Fig. 3.1A). Stimuli were presented in the same order: frontal looms, short translation, receding, loom from above, long translation, 45° right and left, 67.5° right, and loom from below.

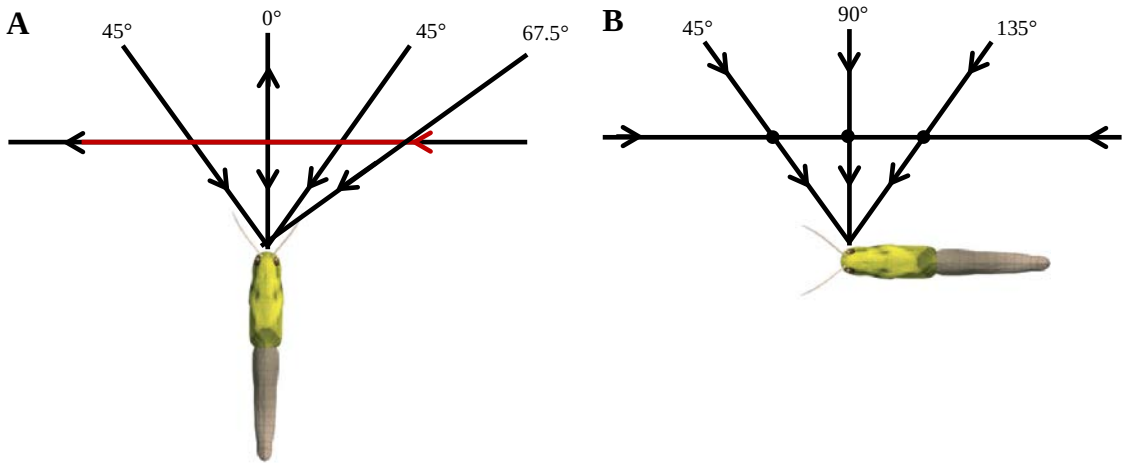

Figure 3.1: Stimulus design. Black disks (7 cm diameter) moved along trajectories that were looming, receding, translating, or transitioned from translating to looming. Trajectories shown are for Experiment 1 (A) and Experiment 2 (B). (A) A total of 14 stimuli were used. Not shown are looms at 45° from above and below. (B) A total of 11 stimuli were used, with a constant $l/|v|$ value of 11.7 ms. Intersections between lines indicate location of potential transitions in trajectory. See text for full description of stimulus trajectories.

3.3.3.2 Experiment 2: Direction and transitions

The second experiment was designed to investigate the response of visual neurons to complex motion. 11 unique trajectories were presented to 20 locusts: translation at 80 cm depth, looming at 45°, 90°, or 135° azimuth, and 3 compound trajectories that began as translating and transitioned to looming at 45°, 90°, or 135° azimuth (Fig. 3.1B). The velocity was held constant at an $l/|v|$ value of 11.7 ms. All trajectories with translational components were repeated for both directions of motion, towards the posterior or towards the anterior. Stimulus order was randomized, with a 90° loom presented at both the beginning and end of stimulus presentation to test for the potential effects of hysteresis caused by the duration of the experiment.

3.3.4 Spike sorting and unit identification

For each stimulus presentation, we recorded and stored neuronal activity data from 4 (Experiment 1) or 8 (Experiment 2) channels, pulses from each frame of the stimulus, and vsync pulses. Neural activity was amplified with an RA16PA Medusa preamp (Tucker-Davis Technologies, Alachua, FL) and sampled at 25 kHz, while vsync and frame pulses were amplified with an RA8GA Loggerhead preamp. An RX5 Pentusa Base Station with Butterworth filter settings of 100 Hz (high pass) and 5 kHz (low pass) was used to store the data to disk. Threshold detection and principle component analysis functions of Offline Sorter (Plexon Inc. Dallas, TX) in combination with manual identification were used to discriminate and sort individual units from raw multichannel data in tetrode configuration (Fig. 3.2). Typically, 5-10 units were found that accounted for 95% of the raw data. Spike times for discriminated units were exported into Neuroexplorer (Nex Techniologies, Plexon Inc., Dallas, TX) and aligned to

either the projected time of collision (TOC) for trajectories with looming components, the time the object crossed 90° azimuth (T90) for translating-only trajectories, or the beginning of presentation for receding stimuli. These were used as reference events to generate peristimulus time histograms (PSTH), which were smoothed with a 50 ms Gaussian filter to estimate changes in firing rate during stimulus presentation. For each discriminated unit, the response profile was described by the amplitude and timing of a peak in firing rate. For Experiment 2, units were also characterized by whether they responded to transitions in trajectory.

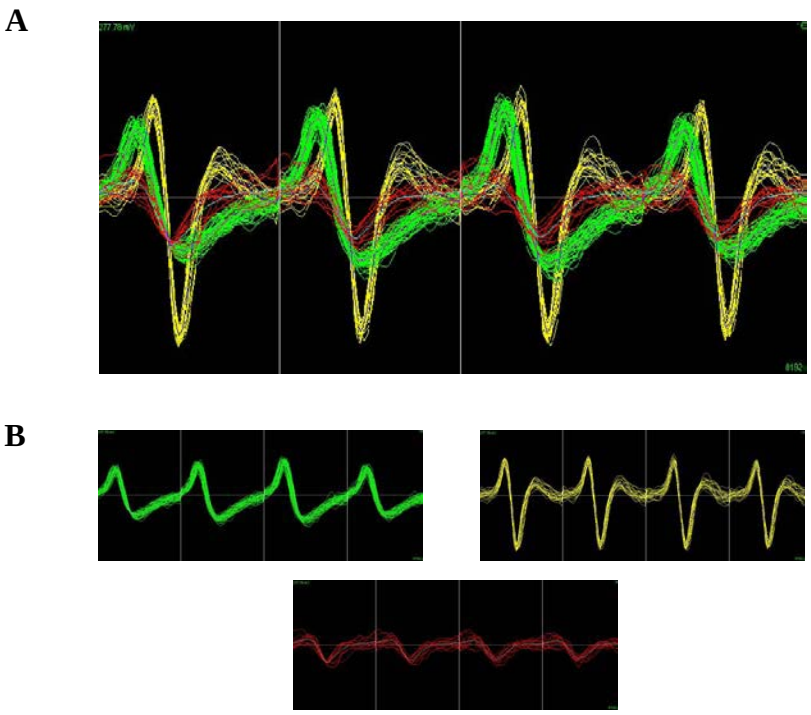

Figure 3.2: Tetrode recordings from the connective of one animal. Each line corresponds with a single action potential recorded from four extracellular recording sites. (A) Overlaid neuronal activity of multiple units. Spikes were sorted through a combination of principle component analysis and manual identification. Colours indicate sorted units. (B) Three units were identified in this recording, based on the shape, direction, and magnitude of the activity.

3.3.5 Data analysis

Discriminated units from all animals were analysed and grouped based on the parameters of their response to each of the 14 (Experiment 1) or 11 (Experiment 2) stimuli. PSTHs were used as a last step to identify units with similar firing patterns for a select few stimuli. Data collected for Experiment 1 and Experiment 2 were analysed independently; disparities in stimulus presentation (i.e. non-randomized order) prevented pooling of data between experiments, even with similar stimuli. To this end, units from Experiment 1 were designated numbers while those from Experiment 2 were designated letters.

After sorting, the groups were plotted using SigmaPlot 10.0 and differences between groups were tested with SigmaStat 3.5 (Systat Software, Richmond, CA). Parametric data were tested with a one-way students t-test, whereas nonparametric data were tested with a Mann-Whitney Rank Sum test. All data were graphed as box plots.

3.4 RESULTS

3.4.1 Velocity and trajectory

An average of 9 +/- 3 units was found in each of 22 animals that showed a response to at least 1 of the 14 stimuli presented for a total of 188 units. These were sorted in to four categories based on common response profiles: 21 were classified as Unit 1, 20 as Unit 2, 11 as Unit 3, and 31 were designated “Other”. The remaining 105 units were not classified due to lack of response to more than 3 stimuli, preventing confident categorization. Several smaller groups with similarities in firing were combined as Other; 4 units appeared to show preference for ipsilateral

looms in comparison to contralateral, and 6 units showed preference to looming from below over looming from above. However, due to the low numbers and lack of other similarities, these could not be reliably classified independently. Despite some similarities to previously describe neurons, differences in response profiles in addition to the inability to discriminate between units based on spike amplitude prohibited conclusive identification of neurons, resulting in the use of Unit X as labels.

The response of all 3 units to a looming stimulus was an increase in the firing rate as the object approached, with a peak just before the time of collision (Fig. 3.2). The average amplitude of the peak in firing rate in response to a frontal loom with an $l/|v|$ value of 32.5 ms was 80.59 +/- 21.88 spikes/s for Unit 1, 42.83 +/- 18.15 spikes/s for Unit 2, and 37.97 +/- 13.91 spikes/s for Unit 3 (Fig. 3.3). The timing of the peak relative to TOC was -0.21 +/- 0.09 s for Unit 1, -0.17 +/- 0.08 s for Unit 2, and -0.20 +/- 0.10 s for Unit 3. The amplitude of the peak was significantly different between Units 1 and 2 (U = 359.00) and Units 1 and 3 (t = 4.81), but not between Units 2 and 3. The timing of the peak was not significantly different between any of the units.

Translating stimuli evoked an increase in firing rate with a peak around T90 for all three units (Fig. 3.2). In response to a disk translating across 154.4° with an $l/|v|$ value of 40 ms, the peak in firing rate for Unit 1 was 63.06 +/- 22.60 spikes/s at 0.068 +/- 0.223 s, 35.11 +/- 16.99 spikes/s at -0.13 +/- 0.46 s for Unit 2, and 53.09 +/- 16.83 spikes/s at 0.056 +/- 0.157 s for Unit 3. The peak in firing rate was significantly higher for Unit 1 than Unit 2 (U = 278.00) and for Unit 3 than Unit 2 (t = -2.575) but not significantly different between Units 1 and 3. The timing of the peak was significantly later for Unit 1 than Unit 2 (U = 215.50), but not between any other pair. Out of the three discriminated units, only Unit 1 had a significant difference in peak firing rate between looming and translating stimuli (U = 301.00).

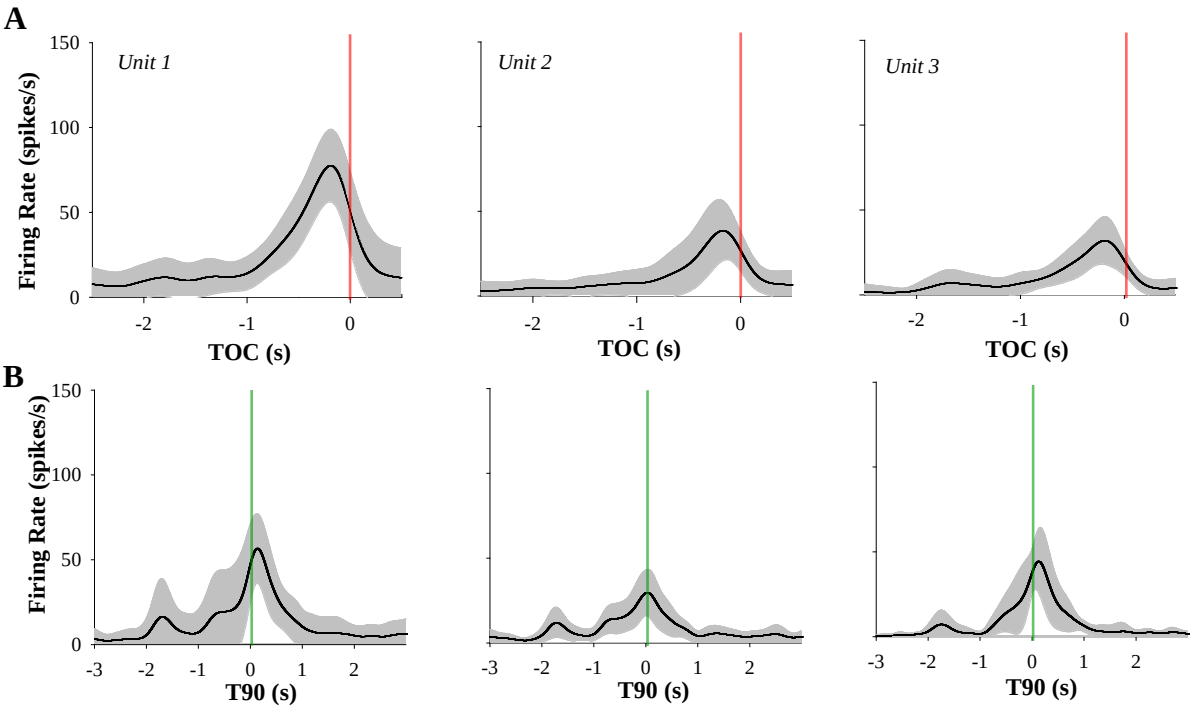

Figure 3.3: Response of three neuronal units to looming (A) and translating (B) visual stimuli. Peristimulus time histograms show the average firing rate from all animals (black) with standard deviation (grey shade) over time relative to TOC (A; red lines) or T90 (B; green lines). (A) The response of all three units to a looming object was an increase in firing rate as the object approached, with a peak just before TOC. Unit 1 responds with the greatest firing rate, while Units 2 and 3 appear similar. (B) All three units responded to a translating object with an increase in firing rate centered around T90. Units 1 and 3 respond most strongly to the stimulus. Note: the peak at approximately -2 s is an artefact of the stimulus initiation.

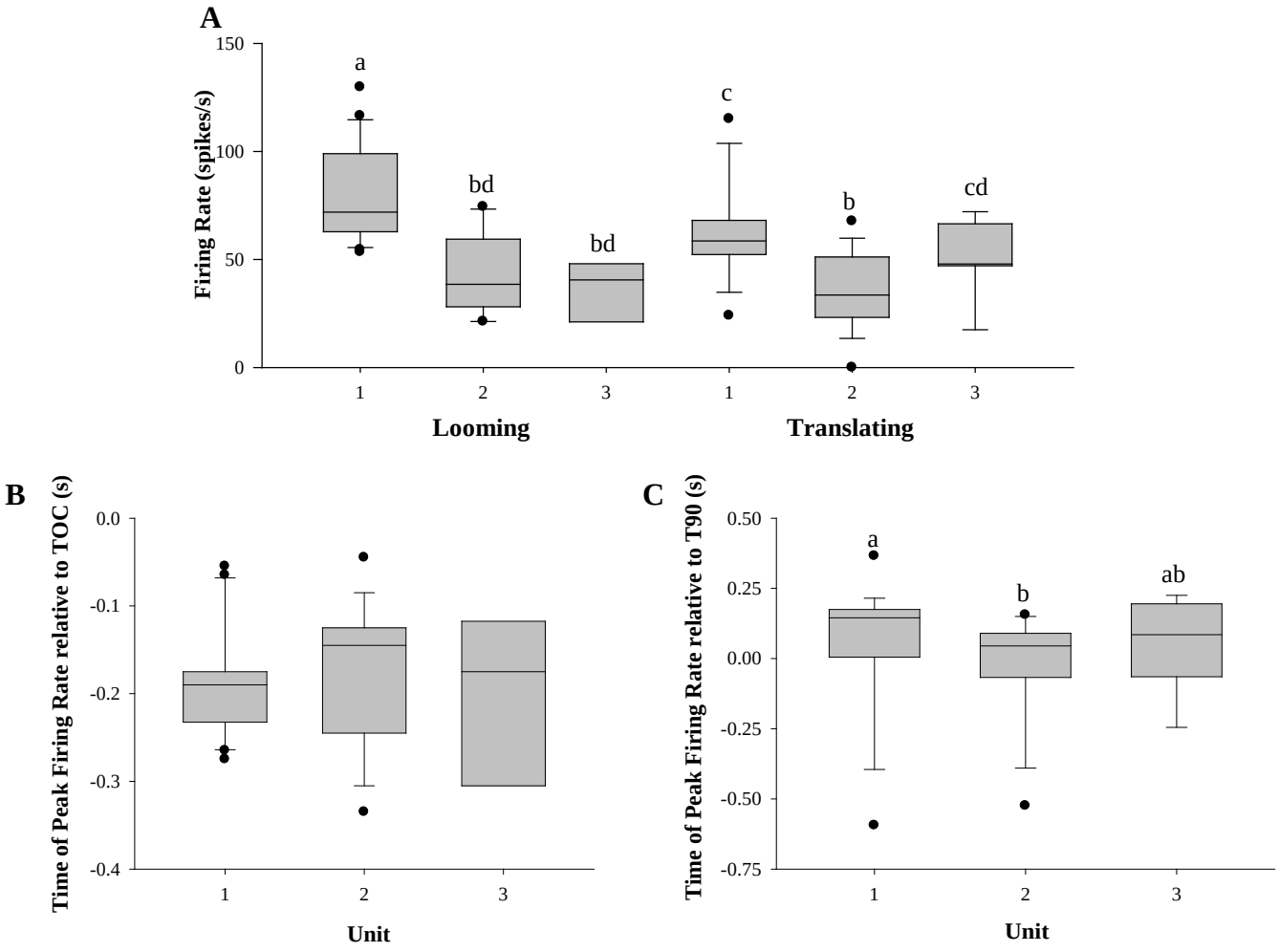

Figure 3.4: Measures of the response of three neuronal units to looming and translating black disks. Boxplots comparing peak firing rate (A) and timing of the peak relative to TOC (B) or T90 (C) are shown. Boxes show 25th and 75th percentiles, with a line at the median, while whiskers indicate the 10th and 90th percentiles, with dots to indicate outliers. (A) Unit 1 showed the most vigorous response to looming disks, while Units 1 and 3 had the greatest firing rate to translating disks. The peak firing rate of Unit 2 was not different in response to looming or translating stimuli. (B) The peak response to looming stimuli occurred before TOC for all units. (C) The peak in firing rate in response to translation was usually after the object crossed 90° azimuth. Unit 2 peaked before Unit 1. Significant difference is shown by different letters. See text for statistics.

3.4.2 Direction and transitions

An average of 3 +/- 1 units were found in 20 *Locusta* that responded to at least one of 11 visual stimuli and did not show the effects of hysteresis. Out of the 61 units identified, 21 were designated Unit A based on similar response profiles, 17 were Unit B, and 8 of the remaining showed responses to multiple stimuli. As in Experiment 1, the remaining units did not respond to enough stimuli to be classified.

The response of both Unit A and Unit B to a disk looming at 90° azimuth was an increase in firing rate that peaked around the time of collision (Fig. 3.5A). The average firing rate at the peak for Unit A was 111.02 +/- 24.83 spikes/s, which was significantly greater than that of Unit B ($t = 7.11$) at 55.02+/- 22.17 spikes/s (Fig. 3.6A). The peak occurred at -0.058 +/- 0.045 s for Unit A, relative to TOC, which was earlier than the peak for Unit B ($U = 40.00$) at 0.034 +/- 0.070 s (Fig. 3.6B).

In response to a translating disk moving posterior, both units gradually increased firing rate around T90, followed by a slow decrease to resting rates (Fig. 3.5B). The average firing rate at the peak for Unit A was 60.33 +/- 40.58 spikes/s, showing considerable variation, while the firing rate for Unit B was 37.34 +/- 19.33 spikes/s (Fig. 3.6C). The peak for Unit A occurred at 0.00 +/- 0.17 s relative to T90, while Unit B peaked at -0.064 +/- 0.246 s (Fig. 3.6D). There was no significant difference in firing rate or timing of the peaks in firing rate between units.

Compound trajectories that transitioned from posterior-directed translation to a loom at 90° azimuth evoked responses similar to a directly looming object, with an increase in firing rate associated with the TOC (Fig. 3.5C). No discernible response to the transition was evident. The peak firing rate for Unit A was 97.11 +/- 25.99 spikes/s, significantly greater than Unit B (t =

6.32) at 43.43 +/- 21.83 spikes/s. The peak occurred at -0.031 +/- 0.064 s relative to TOC for Unit A, which was not significantly different from the peak of Unit B occurring at -0.019 +/- 0.105 s.

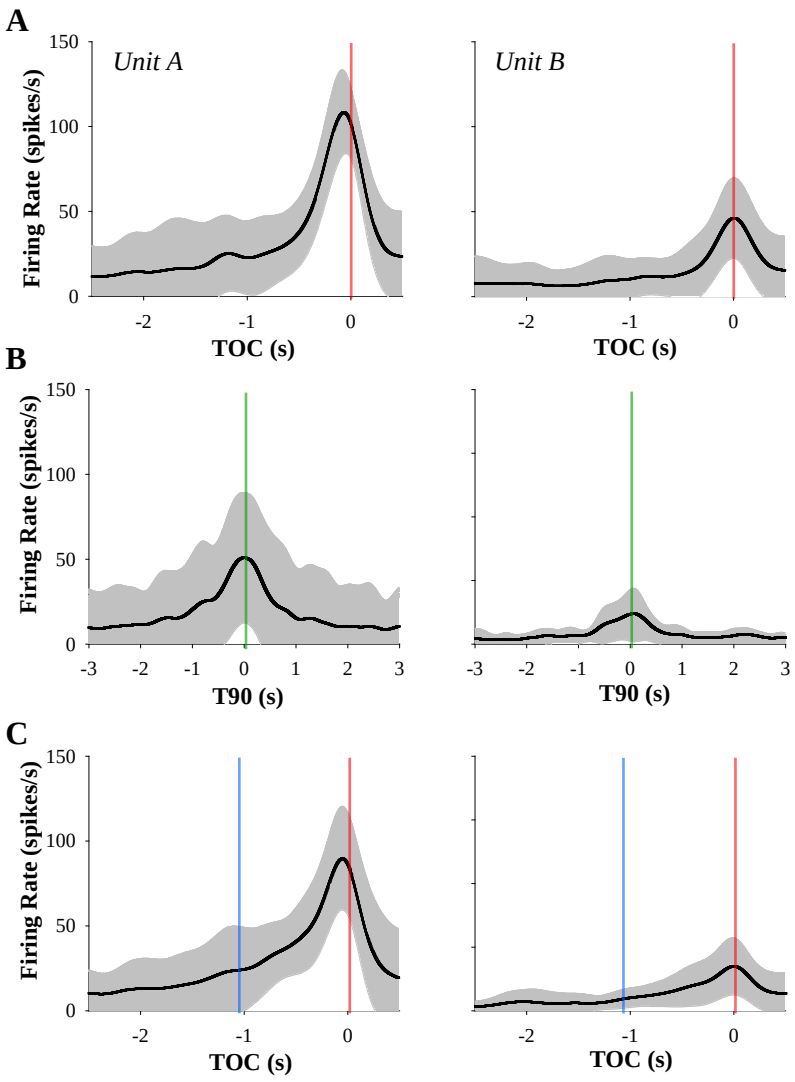

Figure 3.5: Response of two neuronal units to 7 cm diameter black disks on looming (A), translating (B), and compound (C) trajectories. Peristimulus time histograms show the average firing rate (black) and the standard deviation (grey shaded) relative to TOC (A and C; red lines) or T90 (B; green lines). Blue lines indicate the time of transition from translation to looming (TOT). (A) Looming disks evoked an increase in firing rate with a peak associated with the TOC. Unit A had a peak with greater amplitude, while Unit B peaked later. (B) Both units responded to translating disks with an increase in firing rate around T90. There was no difference in peak height or timing between units. Note: Unit A shows considerable variation in response to translation. (C) Compound trajectories evoked responses similar to that of looming trajectories. Unit A responded with a higher amplitude peak, while there was no difference between peak times.

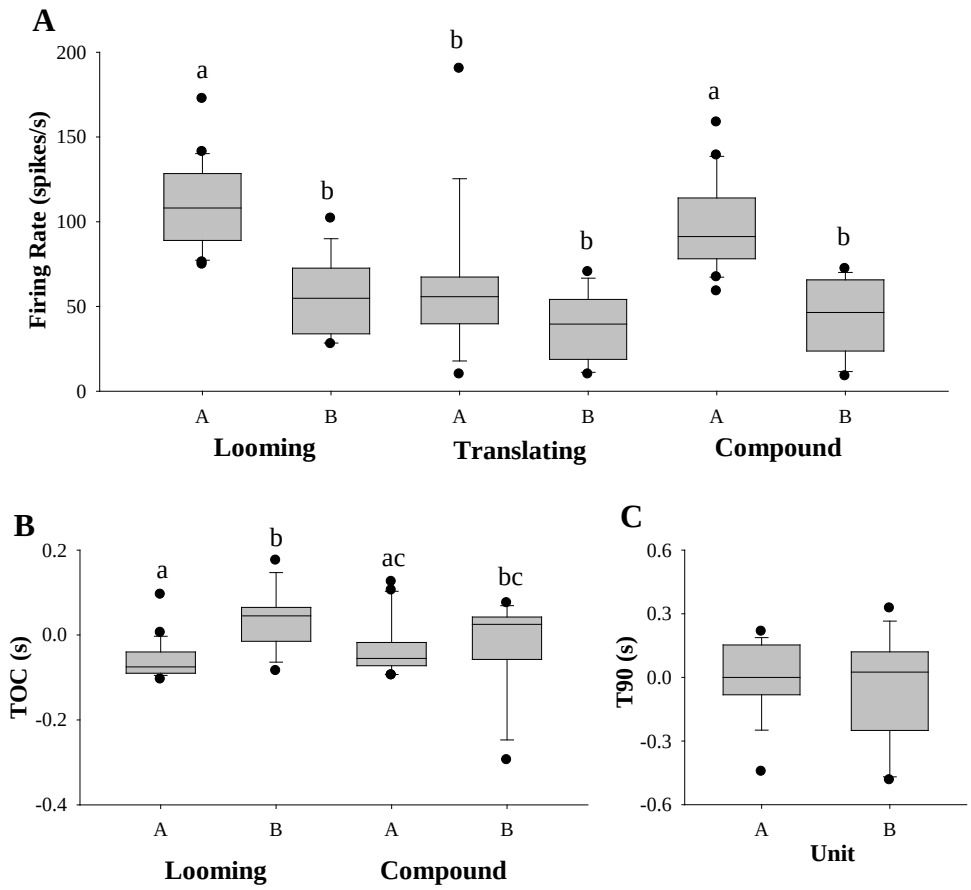

Figure 3.6: Parameters of the response of two neuronal units to looming, translating, and compound trajectories. Boxplots show peak firing rate (A) and peak time relative to TOC (B) or T90 (C). Boxes show 25th and 75th percentiles, with a line at the median, while whiskers indicate the 10th and 90th percentiles, with dots to indicate outliers. (A) Unit A showed a higher peak in firing rate than Unit B to both looming and compound stimuli. No other differences were found. (B) The peak in firing rate for Unit B occurred later in response to looming disks. (C) Both units had a peak in firing rate around T90. Significant differences are shown by different letters. See text for statistics.

For Unit A, the amplitude of the peak in firing rate was significantly greater to looming (U = 331.00) and compound trajectories (U = 362.00) than to translating (Fig. 3.6). However, neither the amplitude nor the timing of the peak was different between looming and compound trajectories (Fig. 3.6). Due to differences in the stimuli, the peak time for translating stimuli was not compared. The peak firing rate of Unit B was only significantly greater in response to

compound trajectories than to translating (t = -2.26). The timing of the peak was not significantly different between looming and compound trajectories.

3.5 DISCUSSION

This preliminary study is one of the first to simultaneously investigate the responses of multiple neurons in the locust system to visual motion. The data collected by Experiment 1 and Experiment 2, described in part here, cover a range of visual stimuli that overlaps almost all previous studies with the DCMD and LGMD. In Experiment 1, we found three neuronal units with unique firing profiles. One of these neurons appears to be looming-sensitive, similar to the DCMD, while another responds preferentially to translation; the third unit responded similarly to both looming and translating stimuli. In Experiment 2, we found two distinct neuronal units which showed some similarities to the DCMD and LDCMD. However, neither showed modulation of firing rate in response to transitions from translation to looming, which is a characteristic of the DCMD (see Chapter 2; (McMillan and Gray, 2012).

3.5.1 Caveats

While this data set contains a large amount of data, there are some confounding factors that must be addressed. As mentioned above, Experiment 1 did not include randomized stimulus presentation. This could result in hysteresis affecting the response to later stimuli due to earlier motion. This is compounded by the unknown characteristics of novel units; while habituation of the DCMD and LDCMD have been described (Gray et al., 2010), other neurons could be more

sensitive. Experiment 1 also lacked a control for the duration of the experiment. Unable to verify consistent response throughout the recording, all data was taken "as-is", which is the primary reason for the discrepancy between number of units identified in Experiment 1 compared to Experiment 2. These caveats, in addition to differences in stimuli used, prevent comparison between experiments, and potentially comparing Experiment 1 to existing literature.

The experiments described here involved the collection of multichannel data from multiple animals. The first step in analysis of this type of data is spike-sorting. Here we used a combination of offline principle component analysis and manual corrections. However, spike-sorting is a complicated and demanding task that may implicitly include bias (Ventura and Gerkin, 2012). Furthermore, organs and muscles of a semi-intact preparation, such as that used here, may introduce biological noise that can confound analysis. This issue is particularly important when one is interested in investigating correlations and synchronous firing across multiple neurons (Pillow et al., 2013); when spikes overlap (as would be expected with synchrony), the resulting waveforms would not be identifiable as either individual unit. For a review of spike sorting algorithms and performance see (Takekawa et al., 2010) and (Einevoll et al., 2012). While we are confident that our methods resulted in discreet neuronal units, mis-sorting could result in units with lower firing rates than actually found due to the splitting of the response of a single unit in to two or more pieces, or higher firing rates in the case of splicing the activity of multiple units together.

3.5.2 Head-on collision and translation

Each of the three units identified in Experiment 1 show unique firing properties. Only Unit 1 responded more to looming than to translating, which it responded to more vigorously than either Units 2 or 3. Unit 3 had a significantly different peak firing rate in response to translation than Unit 2. In combination, these show that each of the units are distinct in their responses to visual stimuli.

The response of Unit 1 to a looming disk was typical of that seen with the DCMD (Rind and Simmons, 1992; Gabbiani et al., 1999; Gray et al., 2001). Previous experiments challenged the DCMD with head-on looms at $l/|v|$ values of 16.7 and 33.3 ms ((Gray et al., 2001), the latter of which evoked a characteristic response with a peak time centered around -0.06 s relative to TOC and a peak frequency above 200 spikes/s. Although the stimuli themselves are similar, these values are different from the parameters of Unit 1 responding to a head-on loom with a comparable $l/|v|$. The only study to identify the LDCMD (Gray et al., 2010) used only repeated presentations of looming disks approaching at 90° azimuth with an $l/|v|$ value of 35 ms, which does not correspond with any of the stimuli used in Experiment 1. This precludes comparisons to any of the units described here. The DIMD, as discussed above, has a response indistinguishable to the DMCD (Fotowat et al., 2009) beyond the differences in preference between ipsilateral and contralateral stimuli. This was briefly investigated for all three units (results not shown), and only Unit 1 showed any preference, which was found to be for contralateral movement. While this suggests that Unit 1 is the DCMD, it prevents Unit 2 or 3 from being the DIMD. For the other visual neurons in the locust system discussed above (i.e. DNI, DNM, and DNC), only wide-field stimuli have been used, so results can not be compared.

3.5.3 Lateral looming, translating, and transitions

Three stimuli were presented here to be used for preliminary identification: a looming, translating, and compound trajectory all with $l/|v|$ values of 11.6 ms. All looming components approached at 90° azimuth, chosen for both the robust DCMD response and for clear identification of transition-associated features (see Chapter 2). When taken individually, both Unit A and B show interesting properties. Unit A responded to looming and translational motion, but was unaffected by transitions in object trajectories. This includes firing rates and times that were not significantly different between looming-only and compound trajectories. Unit B had a peak response to looming objects that was much later in time, with a firing rate that was no different than in response to translating disks. In comparison to Unit A, there is a significant difference in the firing rate evoked by a direct loom, but not by a loom following translation.

Similar to Unit 1 above, Unit A was found to have properties comparable to the DCMD; however, there are again some discrepancies. While the peak timing and firing rate in response to looming and translation are more similar to previous DCMD results (Gabbiani et al., 2002; Gray, 2005), the lack of modulation in the presence of transitions contradicts recent findings (McMillan and Gray, 2012). The response of Unit B appears similar to the LDCMD. In the LDCMD, a looming object with an $l/|v|$ of 35 ms approaching at 90° azimuth evoked a peak firing rate of around 100 spikes/s with a time of -0.15 s relative to collision (Gray et al., 2010). A faster-moving stimulus evoked a lower amplitude peak from Unit B that occurred after the projected time of collision. Studies with the DCMD have found lower $l/|v|$ values, and thus faster moving objects, evoke peaks that are higher and later in time (Gabbiani et al., 2002); while it may not be applicable to the LDCMD, similarities between the DCMD and LDCMD have suggested that their firing rates are correlated.

While the stimuli used in Experiment 2 are different from those in Experiment 1, responses to 45° looms, the most similar stimuli between experiments, seem to suggest that Units A and B are different from the units identified in Experiment 1.

3.5.4 Visually sensitive neurons

The data shown is a subset of the total recorded neuronal responses and visual stimuli. Both experiments combined found almost 250 neuronal units, of which only 92 were categorized by the procedure presented here. The low number classified can be attributed to the difficulty of confidently grouping units that only responded to 2 or 3 stimuli; it is important to note that this does not mean that these units should be discarded. Proper ensemble analysis would be able to identify coincident firing for each unit in every animal and would likely prove to be a much more efficient, and accurate, method of comparison. In addition to identifying individual units, this analysis could discriminate populations that fire in synchrony, and the variability of membership in these populations in regards to the visual environment.

Beyond simple identification, the range in stimuli utilized for both experiments allows for detailed description of any units that are found. The response of one neuron when challenged by the visual motion of either experiment is often sufficient for a publication on its own; when this is expounded to include all that was recorded here, the sheer amount is staggering. Unfortunately, this level of analysis requires first ensemble analysis followed by further detailed characterization, a task that is beyond the scope of a single chapter.

3.5.5 Conclusion

In conclusion, we identified here as many as 5 distinct neuronal units that respond to visual motion. While several show similarities to previously identified neurons, there is also evidence of novel firing properties. Additional units are evident in the data, but due to time constraints in combination with low incidence, these could not be described in more detail here. The data collected for the experiments described here provide enough information to characterize in detail the responses of multiple neurons, both individually and in populations with other neurons, to visual motion. This form of analysis has never been applied to the locust visual system at such a scale, and will lead to a far more detailed description of this system than has been previously possible.

CHAPTER 4

GENERAL DISCUSSION

4.1 ENCODING OF VISUAL INFORMATION

Results from Chapter 2 illustrate the ability of a single neuron to encode complex sensory information to a degree that has not been displayed before in the locust. Through features of the response profile, the DCMD was able to encode information related to transitions from non-looming to looming, the location of these transitions within the locusts' visual field, and the velocity at which the object was moving. This provides evidence for multiplexing within the DCMD. In addition, the data presented supports that the modulation of firing rate at the time of transition is related to changes in expansion properties of a disk, namely instantaneous subtense acceleration and acceleration of the leading edge. However, the DCMD did not appear to encode the velocity of objects that followed trajectories that were solely translational.

Chapter 3 explores the presence of multiple visually-sensitive interneurons in the locust connective. Preliminary results of the first experiment show three units with distinctive patterns of activity in response to objects translating and looming in front of the locust. The parameters of the responses of these units are different both amongst themselves and in comparison to previously described neurons. The second experiment identified two units with unique response profiles to translating, looming, and compound trajectories presented laterally. While the responses to translating and looming were somewhat similar to the DCMD and LDCMD, neither showed the transition-associated modulation that is described of the DCMD in detail in Chapter 2.

Together, Chapters 2 and 3 serve to illuminate the not-yet completely appreciated complexity of the locust visual system. Chapter 2 expands on the capabilities of a single visual neuron to encode complex visual motion beyond what has been previously described. Chapter 3 identifies additional neurons within the same system that respond to visual motion in manners both similar and dissimilar to the DCMD. If the results of both Chapters are taken together, they suggest that the visual system of the locust is incredibly complex.

4.2 IMPLICATIONS FOR BEHAVIOUR

The single pathway formed by the LGMD and DCMD integrates the locusts' entire field of view, and appears to be capable of identifying multiple components of the visual environment that should impact in-flight maneuvers, particularly those with strong influence on survival such as collision avoidance. Through connections with the flight motor neurons that control these behaviours, the DCMD is capable of translating this information in to action. The LGMD/DCMD pathway has been implicated in both collision avoidance flight maneuvers and escape jump behaviours. Parameters of the trajectory of an object should have an effect on the behaviour of an animal; a larger or faster approaching object should elicit behaviours that are earlier in time to allow completion of the maneuver. In contrast, an object that simply passes by, as in translating motion, does not necessitate an immediate response, regardless of the velocity. The results of Chapter 2 support this; while the DCMD modulates the response to looming objects depending on velocity, it does not for translating objects. Compound trajectories are more complicated, but more accurately reflect a natural situation. The translational component does not require behavioural responses, but the location of the object when it begins to loom

could have implications on the necessary response. For example, an oncoming predatory bird may be more easily lost by a quick turn than one approaching from behind.

The implications of any of the units described in Chapter 3 on behaviour are currently unclear. Without understanding the anatomical location and connections the projections of these units make, it is difficult to propose function. The general location, i.e. the connective anterior to prothoracic ganglion, allows many possibilities. Interneurons that appear to respond to visual motion could make connections with motor neurons and directly impact locomotion, similar to the function suggested of the DCMD. However, they could also be part of a feedback system, relaying muscle activity back to the locust brain. To add complications, they could play a regulatory role, influencing the responses of other interneurons, rather than having direct effects. There is a multitude of possibilities for these units, but more firm conclusions would require data that is not yet available.

4.3 FUTURE DIRECTIONS

While both chapters presented here give evidence that the locust visual system is much more complex than has been previously thought, they also open new avenues of research. The neuronal activity described in Chapter 2 requires behavioural studies using similar visual stimuli to correctly correlate results. In addition, as mentioned above, the biophysical mechanisms that underlie the proposed correlation between the change in firing rate at trajectory transition and stimulus parameters has not yet been determined. The results from Chapter 3 do not yet require future experiments; the data collected still requires more in depth analysis. Briefly, these data could be used for ensemble analysis that would identify similar units between animals and

populations within a single animal. The wide array of stimuli that were used allows for detailed description of the response parameters of each of the neurons identified, almost to the degree of the DCMD. At this point, all that is required is time.

REFERENCES

Altman JS, Kien J. Functional organization of the subesophageal ganglion in arthropods. In: *Arthropod Brain*, edited by Gupta AP. New York: Wiley, 1987, p. 265–301.

Baker PS, Gewecke M, Cooter RJ. The natural flight of the migratory locust,Locusta migratoria L. *J. Comp. Physiol.* 141: 233–237, 1981.

Borst A. Drosophila's View on Insect Vision. *Curr. Biol.* 19: R36–R47, 2009.

Brown EN, Frank LM, Tang D, Quirk MC, Wilson MA. A Statistical Paradigm for Neural Spike Train Decoding Applied to Position Prediction from Ensemble Firing Patterns of Rat Hippocampal Place Cells. *J. Neurosci.* 18: 7411–7425, 1998.

Burrows M, Rowell DCHF. Connections between descending visual interneurons and metathoracic motoneurons in the locust. *J. Comp. Physiol.* 85: 221–234, 1973.

Burrows M. Monosynaptic connexions between wing stretch receptors and flight motoneurones of the locust. *J. Exp. Biol.* 62: 189–219, 1975.

Burrows M. *The neurobiology of an insect brain*. Oxford University Press, 1996.

Buzsáki G. Large-scale recording of neuronal ensembles. *Nat. Neurosci.* 7: 446–451, 2004.

Campbell JI. The Anatomy of the Nervous System of the Mesothorax of Locusta Migratoria Migradorioides R. & F. *Proc. Zool. Soc. Lond.* 137: 403–432, 1961.

Card GM. Escape behaviors in insects. *Curr. Opin. Neurobiol.* 22: 180–186, 2012.

Carlson SD, Saint Marie RL. Structure and Function of Insect Glia. *Annu. Rev. Entomol.* 35: 597–621, 1990.

Caveney S, McIntyre P. Design of Graded-Index Lenses in the Superposition Eyes of Scarab Beetles. *Philos. Trans. R. Soc. Lond. B. Biol. Sci.* 294: 589–632, 1981.

Chan RW, Gabbiani F. Collision-avoidance behaviors of minimally restrained flying locusts to looming stimuli. *J. Exp. Biol.* 216: 641–655, 2013.

Chapman RF. A biology of locusts. : [4+] 67pp., 1976.

Chapman RF. *The Insects: Structure and Function*. Cambridge University Press, 1998.

Chase SM, Young ED. First-spike latency information in single neurons increases when referenced to population onset. *Proc. Natl. Acad. Sci.* 104: 5175–5180, 2007.

Clemens IAH, Vrijer MD, Selen LPJ, Gisbergen JAMV, Medendorp WP. Multisensory Processing in Spatial Orientation: An Inverse Probabilistic Approach. *J. Neurosci.* 31: 5365–5377, 2011.

Daw ND, O'Doherty JP, Dayan P, Seymour B, Dolan RJ. Cortical substrates for exploratory decisions in humans. *Nature* 441: 876–879, 2006.

Dawson J, Dawson-Scully K, Robert D, Robertson RM. Forewing asymmetries during auditory avoidance in flying locusts. *J. Exp. Biol.* 200: 2323–2335, 1997.

Domenici P, Blagburn JM, Bacon JP. Animal escapology I: theoretical issues and emerging trends in escape trajectories. *J. Exp. Biol.* 214: 2463–2473, 2011.

Dubuc R, Brocard F, Antri M, Fénelon K, Gariépy J-F, Smetana R, Ménard A, Le Ray D, Viana Di Prisco G, Pearlstein É, Sirota MG, Derjean D, St-Pierre M, Zielinski B, Auclair F, Veilleux D. Initiation of locomotion in lampreys. *Brain Res. Rev.* 57: 172–182, 2008.

Dunbier JR, Wiederman SD, Shoemaker PA, O'Carroll DC. Facilitation of dragonfly target-detecting neurons by slow moving features on continuous paths. *Front. Neural Circuits* 6, 2012.

Eaton RC, Lee RKK, Foreman MB. The Mauthner cell and other identified neurons of the brainstem escape network of fish. *Prog. Neurobiol.* 63: 467–485, 2001.

Einevoll GT, Franke F, Hagen E, Pouzat C, Harris KD. Towards reliable spike-train recordings from thousands of neurons with multielectrodes. *Curr. Opin. Neurobiol.* 22: 11–17, 2012.

Elhilali M, Ma L, Micheyl C, Oxenham A, Shamma S. Rate Versus Temporal Code? A Spatio-Temporal Coherence Model of the Cortical Basis of Streaming [Online]. In: *The Neurophysiological Bases of Auditory Perception*, edited by Lopez-Poveda EA, Palmer AR, Meddis R. Springer New York, p. 497–506. http://link.springer.com/chapter/10.1007/978-1-4419-5686-6_46 [30 Jun. 2013].

Ernst MO, Banks MS. Humans integrate visual and haptic information in a statistically optimal fashion. *Nature* 415: 429–433, 2002.

Felsen G, Dan Y. A natural approach to studying vision. *Nat. Neurosci.* 8: 1643–1646, 2005.

Ferster D, Spruston N. Cracking the Neuronal Code. *Science* 270: 756–757, 1995.

Fotowat H, Fayyazuddin A, Bellen HJ, Gabbiani F. A Novel Neuronal Pathway for Visually Guided Escape in Drosophila melanogaster. *J. Neurophysiol.* 102: 875–885, 2009.

Fotowat H, Gabbiani F. Relationship between the Phases of Sensory and Motor Activity during a Looming-Evoked Multistage Escape Behavior. *J. Neurosci.* 27: 10047–10059, 2007.

Fotowat H, Gabbiani F. Collision Detection as a Model for Sensory-Motor Integration. *Annu. Rev. Neurosci.* 34: 1–19, 2011.

Fotowat H, Harrison RR, Gabbiani F. Multiplexing of Motor Information in the Discharge of a Collision Detecting Neuron during Escape Behaviors. *Neuron* 69: 147–158, 2011.

Freeman WJ. *Societies of Brains: A Study in the Neuroscience of Love and Hate*. Routledge, 1995.

Gabbiani F, Krapp HG, Koch C, Laurent G. Multiplicative computation in a visual neuron sensitive to looming. *Nature* 420: 320–324, 2002.

Gabbiani F, Krapp HG, Laurent G. Computation of Object Approach by a Wide-Field, Motion-Sensitive Neuron. *J. Neurosci.* 19: 1122–1141, 1999.

Gabbiani F, Krapp HG. Spike-Frequency Adaptation and Intrinsic Properties of an Identified, Looming-Sensitive Neuron. *J. Neurophysiol.* 96: 2951–2962, 2006.

Gabbiani F, Mo C, Laurent G. Invariance of Angular Threshold Computation in a Wide-Field Looming-Sensitive Neuron. *J. Neurosci.* 21: 314–329, 2001.

Gettrup E. Sensory Regulation of Wing Twisting in Locusts. *J. Exp. Biol.* 44: 1–16, 1966.

Gibson JJ. Visually controlled locomotion and visual orientation in animals. *Br. J. Psychol.* 49: 182–194, 1958.

Gilbert C, Strausfeld NJ. Small-field neurons associated with oculomotor and optomotor control in muscoid flies: Functional organization. *J. Comp. Neurol.* 316: 72–86, 1992.

Gollisch T, Meister M. Rapid Neural Coding in the Retina with Relative Spike Latencies. *Science* 319: 1108–1111, 2008.

Gonzalez-Bellido PT, Peng H, Yang J, Georgopoulos AP, Olberg RM. Eight pairs of descending visual neurons in the dragonfly give wing motor centers accurate population vector of prey direction. *Proc. Natl. Acad. Sci.* 110: 696–701, 2013.

Gray JR, Blincow E, Robertson RM. A pair of motion-sensitive neurons in the locust encode approaches of a looming object. *J. Comp. Physiol.* 196: 927–938, 2010.

Gray JR, Robertson RM, Lee JK. Activity of descending contralateral movement detector neurons and collision avoidance behaviour in response to head-on visual stimuli in locusts. *J. Comp. Physiol. [A]* 187: 115–129, 2001.

Gray JR. Habituated visual neurons in locusts remain sensitive to novel looming objects. *J. Exp. Biol.* 208: 2515–2532, 2005.

Gray R, Regan DM. Unconfounding the direction of motion in depth, time to passage and rotation rate of an approaching object. *Vision Res.* 46: 2388–2402, 2006.

Griss C, Rowell CHF. Three descending interneurons reporting deviation from course in the locust. *J. Comp. Physiol.* 158: 765–774, 1986.

Guest BB, Gray JR. Responses of a Looming-Sensitive Neuron to Compound and Paired Object Approaches. *J. Neurophysiol.* 95: 1428–1441, 2006.

Hall C, Bell C, Zelick R. Behavioral evidence of a latency code for stimulus intensity in mormyrid electric fish. *J. Comp. Physiol.* 177: 29–39, 1995.

Hardie RC. Phototransduction in Drosophila melanogaster. *J. Exp. Biol.* 204: 3403–3409, 2001.

Harris-Warrick RM, Marder E. Modulation of Neural Networks for Behavior. *Annu. Rev. Neurosci.* 14: 39–57, 1991.

Harvey MA, Saal HP, Dammann JF, Bensmaia SJ. Multiplexing Stimulus Information through Rate and Temporal Codes in Primate Somatosensory Cortex. *PLoS Biol* 11: e1001558, 2013.

Hatsopoulos N, Gabbiani F, Laurent G. Elementary Computation of Object Approach by a Wide-Field Visual Neuron. *Science* 270: 1000–1003, 1995.

Hedrich UBS, Diehl F, Stein W. Gastric and pyloric motor pattern control by a modulatory projection neuron in the intact crab Cancer pagurus. *J. Neurophysiol.* 105: 1671–1680, 2011.

Hemmi JM, Tomsic D. The neuroethology of escape in crabs: from sensory ecology to neurons and back. *Curr. Opin. Neurobiol.* 22: 194–200, 2012.

Homberg U, Christensen TA, Hildebrand JG. Structure and Function of the Deutocerebrum in Insects. *Annu. Rev. Entomol.* 34: 477–501, 1989.

Homberg U. Structure and functions of the central complex in insects. In: *Arthropod Brain*, edited by Gupta AP. New York: Wiley, 1987, p. 347–67.

Homberg U. Neuroarchitecture of the central complex in the brain of the locust Schistocerca gregaria and S. americana as revealed by serotonin immunocytochemistry. *J. Comp. Neurol.* 303: 245–254, 1991.

Hooper SL, Moulins M. Switching of a neuron from one network to another by sensory-induced changes in membrane properties. *Science* 244: 1587–1589, 1989.

Horridge GA. The Separation of Visual Axes in Apposition Compound Eyes. *Philos. Trans. R. Soc. Lond. B. Biol. Sci.* 285: 1–59, 1978.

Huk AC. Multiplexing in the primate motion pathway. *Vision Res.* 62: 173–180, 2012.

Huxter JR, Senior TJ, Allen K, Csicsvari J. Theta phase–specific codes for two-dimensional position, trajectory and heading in the hippocampus. *Nat. Neurosci.* 11: 587–594, 2008.

Judge S, Rind F. The locust DCMD, a movement-detecting neurone tightly tuned to collision trajectories. *J. Exp. Biol.* 200: 2209–2216, 1997.

Killmann F, Gras H, Schürmann F-W. Types, numbers and distribution of synapses on the dendritic tree of an identified visual interneuron in the brain of the locust. *Cell Tissue Res.* 296: 645–665, 1999.

King SM, Cowey A. Defensive responses to looming visual stimuli in monkeys with unilateral striate cortex ablation. *Neuropsychologia* 30: 1017–1024, 1992.

Kirschfeld K. Die projektion der optischen umwelt auf das raster der rhabdomere im komplexauge von Musca. *Exp. Brain Res.* 3: 248–270, 1967.

Knight RT, Eichenbaum H. Multiplexed memories: a view from human cortex. *Nat. Neurosci.* 16: 257–258, 2013.

Körding K. Decision Theory: What "Should" the Nervous System Do? *Science* 318: 606–610, 2007.

Krapp HG, Gabbiani F. Spatial Distribution of Inputs and Local Receptive Field Properties of a Wide-Field, Looming Sensitive Neuron. *J. Neurophysiol.* 93: 2240–2253, 2005.

Land MF, Nilsson D-E. *Animal Eyes*. Oxford University Press, 2012.

Laughlin SB, Sejnowski TJ. Communication in Neuronal Networks. *Science* 301: 1870–1874, 2003.

Laughlin SB. Neural principles in the peripheral visual systems of invertebrates. In: *Handbook of Sensory Physiology*, edited by Autrum H. Berlin: Springer-Verlag, 1981, p. 133–280.

Lee Y-J, Nordström K. Higher-order motion sensitivity in fly visual circuits. *Proc. Natl. Acad. Sci.* 109: 8758–8763, 2012.

Leutgeb S, Leutgeb JK, Barnes CA, Moser EI, McNaughton BL, Moser M-B. Independent Codes for Spatial and Episodic Memory in Hippocampal Neuronal Ensembles. *Science* 309: 619–623, 2005.

Lisman JE, Jensen O. The Theta-Gamma Neural Code. *Neuron* 77: 1002–1016, 2013.

Liu Y-J, Wang Q, Li B. Neuronal Responses to Looming Objects in the Superior Colliculus of the Cat. *Brain. Behav. Evol.* 77: 193–205, 2011.

Lochmann T, Deneve S. Neural processing as causal inference. *Curr. Opin. Neurobiol.* 21: 774–781, 2011.

Ma Z, Guo W, Guo X, Wang X, Kang L. Modulation of behavioral phase changes of the migratory locust by the catecholamine metabolic pathway. *Proc. Natl. Acad. Sci.* 108: 3882–3887, 2011.

Maier JX, Neuhoff JG, Logothetis NK, Ghazanfar AA. Multisensory Integration of Looming Signals by Rhesus Monkeys. *Neuron* 43: 177–181, 2004.

Marden JH. Variability in the Size, Composition, and Function of Insect Flight Muscles. *Annu. Rev. Physiol.* 62: 157–178, 2000.

Markram H, Lübke J, Frotscher M, Sakmann B. Regulation of Synaptic Efficacy by Coincidence of Postsynaptic APs and EPSPs. *Science* 275: 213–215, 1997.

Marsat G, Pollack GS. A Behavioral Role for Feature Detection by Sensory Bursts. *J. Neurosci.* 26: 10542–10547, 2006.

Masquelier T, Hugues E, Deco G, Thorpe SJ. Oscillations, Phase-of-Firing Coding, and Spike Timing-Dependent Plasticity: An Efficient Learning Scheme. *J. Neurosci.* 29: 13484–13493, 2009.

Matheson T, Rogers SM, Krapp HG. Plasticity in the Visual System Is Correlated With a Change in Lifestyle of Solitarious and Gregarious Locusts. *J. Neurophysiol.* 91: 1–12, 2004.

McMillan GA, Gray JR. A looming-sensitive pathway responds to changes in the trajectory of object motion. *J. Neurophysiol.* 108: 1052–1068, 2012.

McMillan GA, Loessin V, Gray JR. Bilateral flight muscle activity predicts wing kinematics and 3-dimensional body orientation of locusts responding to looming objects. *J. Exp. Biol.* (June 4, 2013). doi: 10.1242/jeb.087775.

McNaughton BL, O'Keefe J, Barnes CA. The stereotrode: A new technique for simultaneous isolation of several single units in the central nervous system from multiple unit records. *J. Neurosci. Methods* 8: 391–397, 1983.

Medan V, Oliva D, Tomsic D. Characterization of Lobula Giant Neurons Responsive to Visual Stimuli That Elicit Escape Behaviors in the Crab Chasmagnathus. *J. Neurophysiol.* 98: 2414–2428, 2007.

Mehta MR, Lee AK, Wilson MA. Role of experience and oscillations in transforming a rate code into a temporal code. *Nature* 417: 741–746, 2002.

Miall RC. Visual control of steering in locust flight: the effects of head movement on responses to roll stimuli. *J. Comp. Physiol.* 166: 735–744, 1990.

Mineault PJ, Khawaja FA, Butts DA, Pack CC. Hierarchical processing of complex motion along the primate dorsal visual pathway. *Proc. Natl. Acad. Sci.* 109: E972–E980, 2012.

Möhl B. The role of proprioception in locust flight control. *J. Comp. Physiol.* 156: 103–116, 1985.

Nordstrom K, Barnett PD, O'Carroll DC. Insect Detection of Small Targets Moving in Visual Clutter. *PLoS Biol.* 4, 2006.

O'Connell MN, Falchier A, McGinnis T, Schroeder CE, Lakatos P. Dual Mechanism of Neuronal Ensemble Inhibition in Primary Auditory Cortex. *Neuron* 69: 805–817, 2011.

O'Day PM, Bacigalupo J, Vergara C, Haab JE. Current issues in invertebrate phototransduction. *Mol. Neurobiol.* 15: 41–63, 1997.

O'shea M, Rowell CHF, Williams JLD. The Anatomy of a Locust Visual Interneurone; the Descending Contralateral Movement Detector. *J. Exp. Biol.* 60: 1–12, 1974.

Oliva D, Tomsic D. Visuo-motor transformations involved in the escape response to looming stimuli in the crab Neohelice (=Chasmagnathus) granulata. *J. Exp. Biol.* 215: 3488–3500, 2012.

Palka J. An inhibitory process influencing visual responses in a fibre of the ventral nerve cord of locusts. *J. Insect Physiol.* 13: 235–248, 1967.

Palop JJ, Mucke L. Amyloid-β-induced neuronal dysfunction in Alzheimer's disease: from synapses toward neural networks. *Nat. Neurosci.* 13: 812–818, 2010.

Panzeri S, Brunel N, Logothetis NK, Kayser C. Sensory neural codes using multiplexed temporal scales. *Trends Neurosci.* 33: 111–120, 2010.

Peron S, Gabbiani F. Spike frequency adaptation mediates looming stimulus selectivity in a collision-detecting neuron. *Nat. Neurosci.* 12: 318–326, 2009a.

Peron SP, Gabbiani F. Role of spike-frequency adaptation in shaping neuronal response to dynamic stimuli. *Biol. Cybern.* 100: 505–520, 2009b.

Peron SP, Jones PW, Gabbiani F. Precise Subcellular Input Retinotopy and Its Computational Consequences in an Identified Visual Interneuron. *Neuron* 63: 830–842, 2009.

Peron SP, Krapp HG, Gabbiani F. Influence of Electrotonic Structure and Synaptic Mapping on the Receptive Field Properties of a Collision-Detecting Neuron. *J. Neurophysiol.* 97: 159–177, 2007.

Pillow JW, Shlens J, Chichilnisky EJ, Simoncelli EP. A Model-Based Spike Sorting Algorithm for Removing Correlation Artifacts in Multi-Neuron Recordings. *PLoS ONE* 8: e62123, 2013.

Pinter RB, Olberg RM, Abrams TW. Is the Locust DCMD A Looming Detector? *J. Exp. Biol.* 101: 327–331, 1982.

Pinter RB. The electrophysiological bases for linear and for nonlinear product term lateral inhibition and the consequences for wide field textured stimuli. *J. Theor. Biol.* 105: 233–243, 1983.

Rind FC, Bramwell DI. Neural network based on the input organization of an identified neuron signaling impending collision. *J. Neurophysiol.* 75: 967–985, 1996.

Rind FC, Santer RD, Wright GA. Arousal Facilitates Collision Avoidance Mediated by a Looming Sensitive Visual Neuron in a Flying Locust. *J. Neurophysiol.* 100: 670–680, 2008.

Rind FC, Santer RD. Collision avoidance and a looming sensitive neuron: size matters but biggest is not necessarily best. *Proc. R. Soc. Lond. B Biol. Sci.* 271: S27–S29, 2004.

Rind FC, Simmons PJ. Orthopteran DCMD neuron: a reevaluation of responses to moving objects. I. Selective responses to approaching objects. *J. Neurophysiol.* 68: 1654–1666, 1992.

Rind FC. A chemical synapse between two motion detecting neurones in the locust brain. *J. Exp. Biol.* 110: 143–167, 1984.

Rind FC. Non-directional, movement sensitive neurones of the locust optic lobe. *J. Comp. Physiol.* 161: 477–494, 1987.

Rind FC. Intracellular characterization of neurons in the locust brain signaling impending collision. *J. Neurophysiol.* 75: 986–995, 1996.

Robert D, Rowell CHF. Locust flight steering. *J. Comp. Physiol.* 171: 41–51, 1992.

Robertson R, Kuhnert C, Dawson J. Thermal avoidance during flight in the locust Locusta migratoria. *J. Exp. Biol.* 199: 1383–1393, 1996.

Robertson RM, Johnson AG. Collision Avoidance of Flying Locusts: Steering Torques and Behaviour. *J. Exp. Biol.* 183: 35–60, 1993a.

Robertson RM, Johnson AG. Retinal image size triggers obstacle avoidance in flying locusts. *Naturwissenschaften* 80: 176–178, 1993b.

Robertson RM, Reye DN. Wing Movements Associated with Collisionavoidance Manoeuvres During Flight in the Locust Locusta Migratoria. *J. Exp. Biol.* 163: 231–258, 1992.

Roeder KD. Neural factors and evitability in insect behavior. *J. Exp. Zool.* 194: 75–88, 1975.

Roessingh P, Simpson SJ, James S. Analysis of Phase-Related Changes in Behaviour of Desert Locust Nymphs. *Proc. R. Soc. Lond. B Biol. Sci.* 252: 43–49, 1993.

Rogers SM, Harston GWJ, Kilburn-Toppin F, Matheson T, Burrows M, Gabbiani F, Krapp HG. Spatiotemporal Receptive Field Properties of a Looming-Sensitive Neuron in Solitarious and Gregarious Phases of the Desert Locust. *J. Neurophysiol.* 103: 779–792, 2010.

Rowell CF, O'Shea M, Williams JL. The neuronal basis of a sensory analyser, the acridid movement detector system. IV. The preference for small field stimuli. *J. Exp. Biol.* 68: 157–185, 1977.

Rowell CHF, Reichert H. Three descending interneurons reporting deviation from course in the locust. *J. Comp. Physiol.* 158: 775–794, 1986.

Rowell CHF. The orthopteran descending movement detector (DMD) neurones: a characterisation and review. *Z. Für Vgl. Physiol.* 73: 167–194, 1971.

Santer RD, Rind FC, Simmons PJ. Predator versus Prey: Locust Looming-Detector Neuron and Behavioural Responses to Stimuli Representing Attacking Bird Predators. *PLoS ONE* 7: e50146, 2012.

Santer RD, Rind FC, Stafford R, Simmons PJ. Role of an Identified Looming-Sensitive Neuron in Triggering a Flying Locust's Escape. *J. Neurophysiol.* 95: 3391–3400, 2006.

Santer RD, Simmons PJ, Rind FC. Gliding behaviour elicited by lateral looming stimuli in flying locusts. *J. Comp. Physiol.* 191: 61–73, 2004.

Santer RD, Yamawaki Y, Rind FC, Simmons PJ. Preparing for escape: an examination of the role of the DCMD neuron in locust escape jumps. *J. Comp. Physiol.* 194: 69–77, 2008.

Schlotterer GR. Response of the locust descending movement detector neuron to rapidly approaching and withdrawing visual stimuli. *Can. J. Zool.* 55: 1372–1376, 1977.

Schurmann F-W. The architecture of the mushroom bodies and related neuropils in the insect brain. In: *Arthropod Brain*, edited by Gupta AP. New York: Wiley, 1987, p. 231–64.

Shadlen MN, Newsome WT. The Variable Discharge of Cortical Neurons: Implications for Connectivity, Computation, and Information Coding. *J. Neurosci.* 18: 3870–3896, 1998.

Shoemaker KL, Robertson RM. Flight motor patterns of locusts responding to thermal stimuli. *J. Comp. Physiol.* 183: 477–488, 1998.

Simmons P. Connexions Between a Movement-Detecting Visual Interneurone and Flight Motoneurones of a Locust. *J. Exp. Biol.* 86: 87–97, 1980a.

Simmons P. A Locust Wind and Ocellar Brain Neurone. *J. Exp. Biol.* 85: 281–294, 1980b.

Simmons PJ. Adaptation and responses to changes in illumination by second- and third-order neurones of locust ocelli. *J. Comp. Physiol.* 173: 635–648, 1993.

Simpson SJ, Despland E, Hägele BF, Dodgson T. Gregarious behavior in desert locusts is evoked by touching their back legs. *Proc. Natl. Acad. Sci.* 98: 3895–3897, 2001.

Snodgrass RE. The thoracic mechanism of a grasshopper, and its antecedents. *Smithson. Misc. Collect.* 82: 1–111, 1929.

Stein RB, Gossen ER, Jones KE. Neuronal variability: noise or part of the signal? *Nat. Rev. Neurosci.* 6: 389–397, 2005.

Storchi R, Bale MR, Biella GEM, Petersen RS. Comparison of latency and rate coding for the direction of whisker deflection in the subcortical somatosensory pathway. *J. Neurophysiol.* 108: 1810–1821, 2012.

Straw AD. Vision Egg: an Open-Source Library for Realtime Visual Stimulus Generation. *Front. Neuroinformatics* 2, 2008.

Sun H, Frost BJ. Computation of different optical variables of looming objects in pigeon nucleus rotundus neurons. *Nat. Neurosci.* 1: 296–303, 1998.

Takekawa T, Isomura Y, Fukai T. Accurate spike sorting for multi-unit recordings. *Eur. J. Neurosci.* 31: 263–272, 2010.

Taube JS. Interspike Interval Analyses Reveal Irregular Firing Patterns at Short, But Not Long, Intervals in Rat Head Direction Cells. *J. Neurophysiol.* 104: 1635–1648, 2010.

Thomas JG. The abdomen of the female desert locust (Schiztocerca gregaria Forskal) with special reference to the sense organs. *Anti-Locust Bull.* 42: 20, 1965.

Uvarov B. Grasshoppers and locusts. A handbook of general acridology. Volume 2. Behaviour, ecology, biogeography, population dynamics. .

Vallis LA, McFadyen BJ. Children use different anticipatory control strategies than adults to circumvent an obstacle in the travel path. *Exp. Brain Res.* 167: 119–127, 2005.

Ventura V, Gerkin RC. Accurately estimating neuronal correlation requires a new spike-sorting paradigm. *Proc. Natl. Acad. Sci.* 109: 7230–7235, 2012.

Walker KMM, Bizley JK, King AJ, Schnupp JWH. Multiplexed and Robust Representations of Sound Features in Auditory Cortex. *J. Neurosci.* 31: 14565–14576, 2011.

Wilson DM, Weis-Fogh T. Patterned Activity of Co-Ordinated Motor Units, Studied in Flying Locusts. *J. Exp. Biol.* 39: 643–667, 1962.

Wolf H. The Locust Tegula: Significance for Flight Rhythm Generation, Wing Movement Control and Aerodynamic Force Production. *J. Exp. Biol.* 182: 229–253, 1993.

Wu L-Q, Niu Y-Q, Yang J, Wang S-R. Tectal neurons signal impending collision of looming objects in the pigeon. *Eur. J. Neurosci.* 22: 2325–2331, 2005.

Yamamoto K, Nakata M, Nakagawa H. Input and Output Characteristics of Collision Avoidance Behavior in the Frog *Rana catesbeiana*. *Brain. Behav. Evol.* 62: 201–211, 2003.

Zupanc GKH. *Behavioral Neurobiology: An Integrative Approach*. Oxford University Press, 2010.